PMR 5251

Assessment of Mechanical Behavior of Materials using Machine Learning Approach

Profa.Dra. Izabel Fernanda Machado and

Profa. Dra. Larissa Driemeier

Profa. Izabel Machado - machadoi@usp.br

Profa. Larissa Driemeier - driemeie@usp.br

Schedule

Schedule	Course program	Prof.
17/09	Relationship between microstructure, mechanical properties and mechanical behavior – Review and point out the most relevant parameters relate to the mechanical behavior of materials using the microstructural features approach	Izabel
24/09	Techniques to evaluating and quantify microstructure features - Present tools for experimental characterization of mechanical properties and microstructural features of materials	Izabel
01/10	Introduce Machine Learning main concepts	Larissa
08/10	Mechanical behavior - stress-strain constitutive equations, workhardening, effect of strain rate, temperature, state of stress, time dependent and independent deformation	Izabel
15/10	Neural Networks in structural analysis	Larissa
22/10	Multiscale analysis	Izabel
29/10	Regression in multiscale problems	Larissa
05/11	Damage and Failure analysis – microstructure heterogeneities stress intensifiers, nucleation and growth of cracks	Izabel
12/11	Classification applied to failure analysis	Larissa
19/11	Seminars	Izabel/Larissa
26/11	Seminars	Izabel/Larissa
03/12	Final Test	Izabel/Larissa

Introduce yourself !

Name

PhD or Master degree candidate (regular or especial)

Advisor

Research approach

Seminar teams and theme (paper) selection

Key words: mechanical behavior and machine learning

Materials Selection in Mechanical Design Third Edition- Ashby

Materials

Table 4.1 Material families and classes

Family	Classes	Short name
Metals (the metals and alloys of engineering)	Aluminum alloys	Al alloys
	Copper alloys	Cu alloys
	Lead alloys	Lead alloys
	Magnesium alloys	Mg alloys
	Nickel alloys	Ni alloys
	Carbon steels	Steels
	Stainless steels	Stainless steels
	Tin alloys	Tin alloys
	Titanium alloys	Ti alloys
	Tungsten alloys	W alloys
	Lead alloys	Pb alloys
	Zinc alloys	Zn alloys
Ceramics	Alumina	Al_2O_3
Technical ceramics (fine ceramics capable of load-bearing application)	Aluminum nitride	AlN
	Boron carbide	B_4C
	Silicon Carbide	SiC
	Silicon Nitride	Si_3N_4
	Tungsten carbide	WC
Non-technical ceramics (porous ceramics of construction)	Brick	Brick
	Concrete	Concrete
	Stone	Stone
Glasses	Soda-lime glass	Soda-lime glass
	Borosilicate glass	Borosilicate glass
	Silica glass	Silica glass
	Glass ceramic	Glass ceramic
Polymers (the thermoplastics and thermosets of engineering)	Acrylonitrile butadiene styrene	ABS
	Cellulose polymers	CA
	Ionomers	Ionomers
	Epoxies	Epoxy
	Phenolics	Phenolics
	Polyamides (nylons)	PA
	Polycarbonate	PC
	Polyesters	Polyester
	Polyetheretherkeytone	PEEK
	Polyethylene	PE
	Polyethylene terephalate	PET or PETE
	Polymethylmethacrylate	PMMA
	Polyoxymethylene (Acetal)	POM
	Polypropylene	PP
	Polystyrene	PS
	Polytetrafluorethylene	PTFE
	Polyvinylchloride	PVC

Table 4.1 (*Continued*)

Family	Classes	Short name
Elastomers (engineering rubbers, natural and synthetic)	Butyl rubber	Butyl rubber
	EVA	EVA
	Isoprene	Isoprene
	Natural rubber	Natural rubber
	Polychloroprene (Neoprene)	Neoprene
	Polyurethane	PU
	Silicone elastomers	Silicones
Hybrids	Carbon-fiber reinforced polymers	CFRP
Composites	Glass-fiber reinforced polymers	GFRP
	SiC reinforced aluminum	Al-SiC
Foams	Flexible polymer foams	Flexible foams
	Rigid polymer foams	Rigid foams
Natural materials	Cork	Cork
	Bamboo	Bamboo
	Wood	Wood

Materials Properties

PMR 5251

Table 3.1 Basic design-limiting material properties and their usual SI units*

Class	Property	Symbol and units	
General	Density	ρ	(kg/m^3 or Mg/m^3)
	Price	C_m	($/kg)
Mechanical	Elastic moduli (Young's, shear, bulk)	E, G, K	(GPa)
	Yield strength	σ_y	(MPa)
	Ultimate strength	σ_u	(MPa)
	Compressive strength	σ_c	(MPa)
	Failure strength	σ_f	(MPa)
	Hardness	H	(Vickers)
	Elongation	ε	(–)
	Fatigue endurance limit	σ_e	(MPa)
	Fracture toughness	K_{1C}	(MPa.m$^{1/2}$)
	Toughness	G_{1C}	(kJ/m^2)
	Loss coefficient (damping capacity)	η	(–)
Thermal	Melting point	T_m	(C or K)
	Glass temperature	T_g	(C or K)
	Maximum service temperature	T_{max}	(C or K)
	Minimum service temperature	T_{max}	(C or K)
	Thermal conductivity	λ	(W/m.K)
	Specific heat	C_p	(J/kg.K)
	Thermal expansion coefficient	α	(K^{-1})
	Thermal shock resistance	ΔT_s	(C or K)
Electrical	Electrical resistivity	ρ_e	(Ω.m or $\mu\Omega$.cm)
	Dielectric constant	ε_d	(–)
	Breakdown potential	V_b	(10^6 V/m)
	Power factor	P	(–)
Optical	Optical, transparent, translucent, opaque	Yes/No	
	Refractive index	n	(–)
Eco-properties	Energy/kg to extract material	E_f	(MJ/kg)
	CO_2/kg to extract material	CO_2	(kg/kg)
Environmental resistance	Oxidation rates	Very low, low, average, high, very high	
	Corrosion rates		
	Wear rate constant	K_A	MPa^{-1}

* Conversion factors to imperial and cgs units appear inside the back and front covers of this book.

Mechanical Properties definition (?):

Characteristics that indicate the elastic or inelastic behavior of a material under pressure (force), such as bending, brittleness, elongation, hardness, and tensile strength.
http://www.businessdictionary.com/definition/mechanical-properties.html

Definition. **Mechanical properties** are physical **properties** that a material exhibits upon the application of forces. Examples of **mechanical properties** are the modulus of elasticity, tensile **strength**, elongation, hardness and fatigue limit.
https://www.nature.com/subjects/mechanical-properties

The mechanical properties of a material are those properties that involve a reaction to an applied load. The mechanical properties of metals determine the range of usefulness of a material and establish the service life that can be expected. Mechanical properties are also used to help classify and identify material. The most common properties considered are strength, ductility, hardness, impact resistance, and fracture toughness.
https://www.nde-ed.org/EducationResources/CommunityCollege/Materials/Mechanical/Mechanical.htm

Mechanical Tests and Specimens

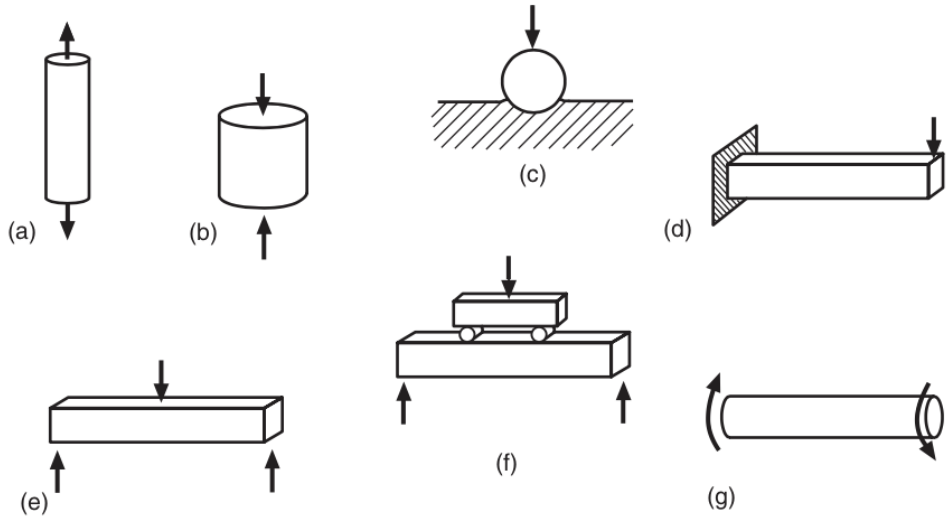

Figure 4.1 Geometry and loading situations commonly employed in mechanical testing of materials: (a) tension, (b) compression, (c) indentation hardness, (d) cantilever bending, (e) three-point bending, (f) four-point bending, and (g) torsion.

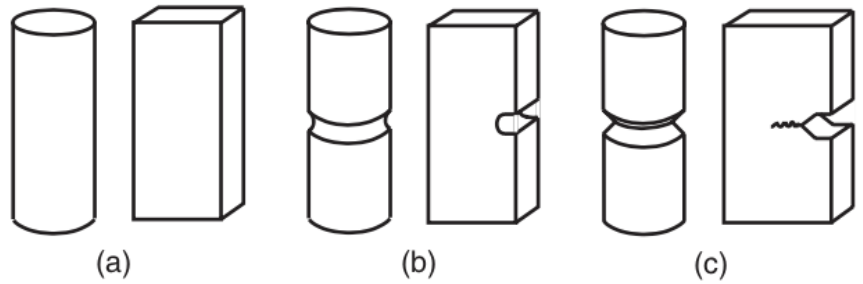

Figure 4.2 Three classes of test specimen: (a) smooth or unnotched, (b) notched, and (c) precracked.

Tensile Test

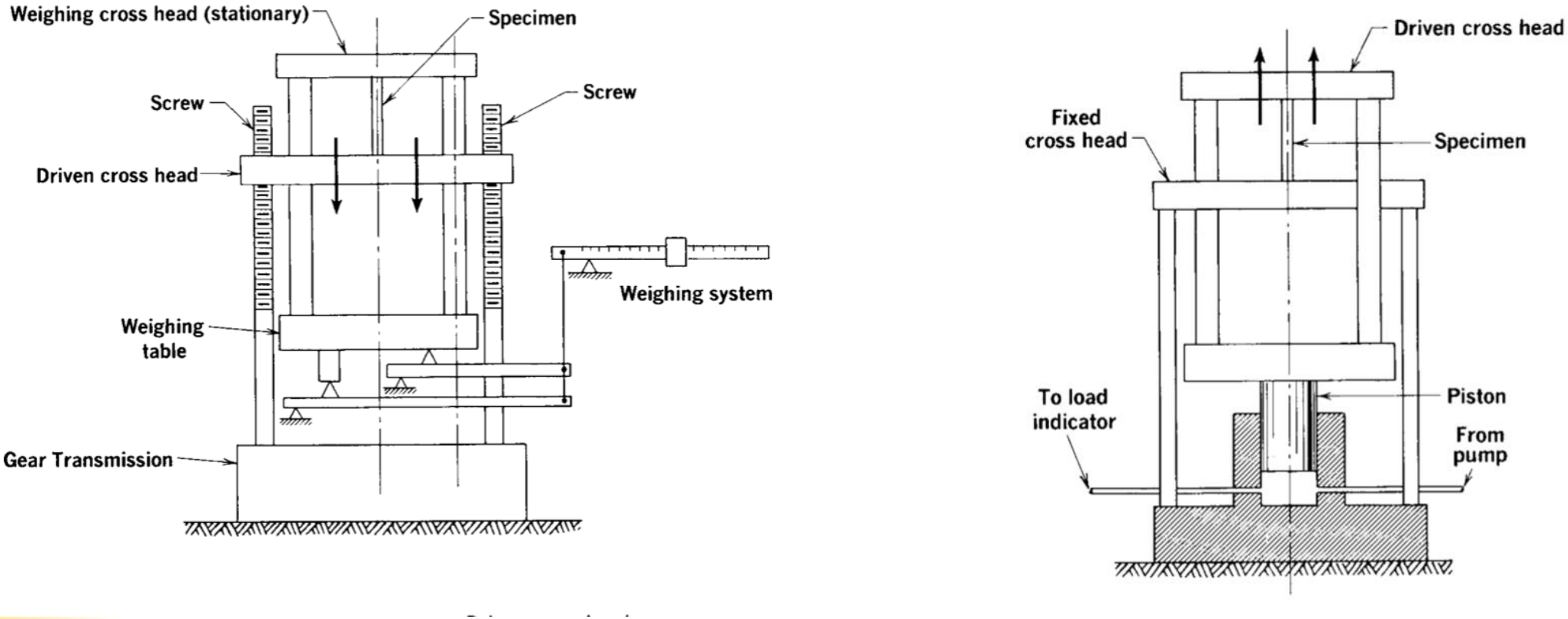

Figure 4.3 Schematics of two relatively simple testing machine designs, called universal testing machines. The mechanical system (top) drives two large screws to apply the force, and the hydraulic system (bottom) uses the pressure of oil in a piston. (From [Richards 61] p. 114; reprinted by permission of PWS-Kent Publishing Co., Boston, MA.)

Tensile Test

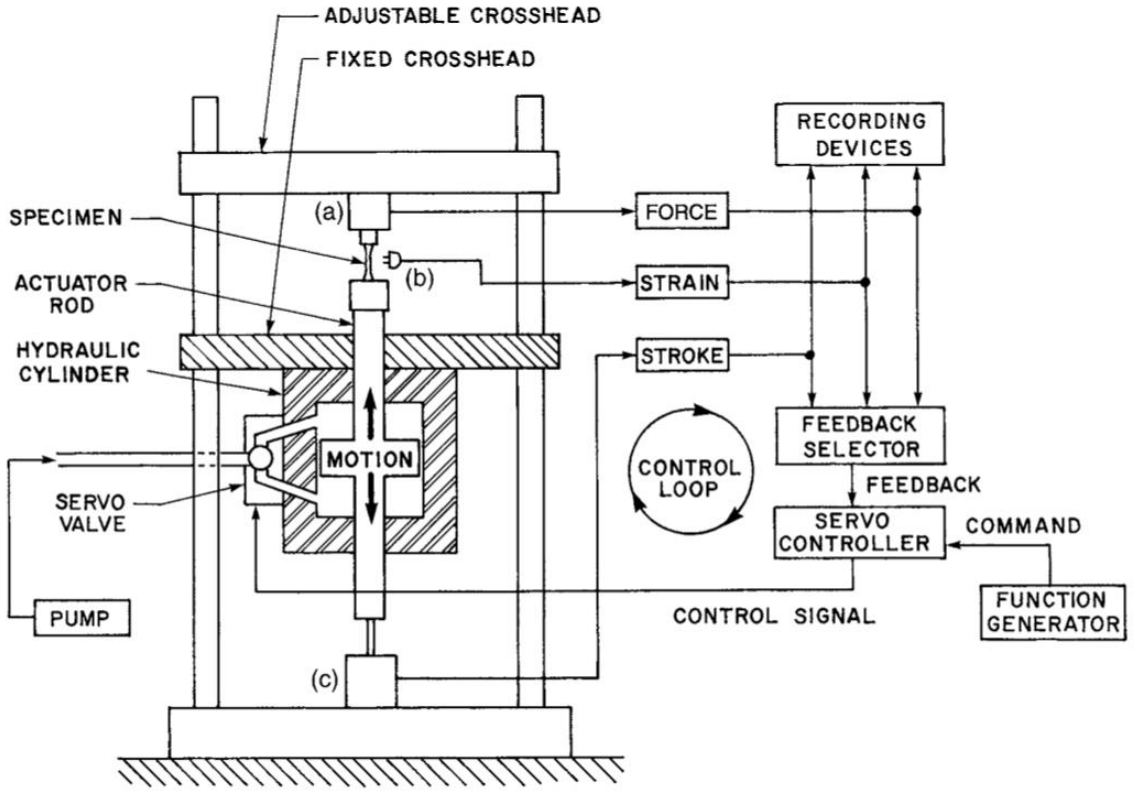

Figure 4.4 Modern closed-loop servohydraulic testing system. Three sensors are employed: (a) load cell, (b) extensometer, and (c) LVDT. (Adapted from [Richards 70]; used with permission.)

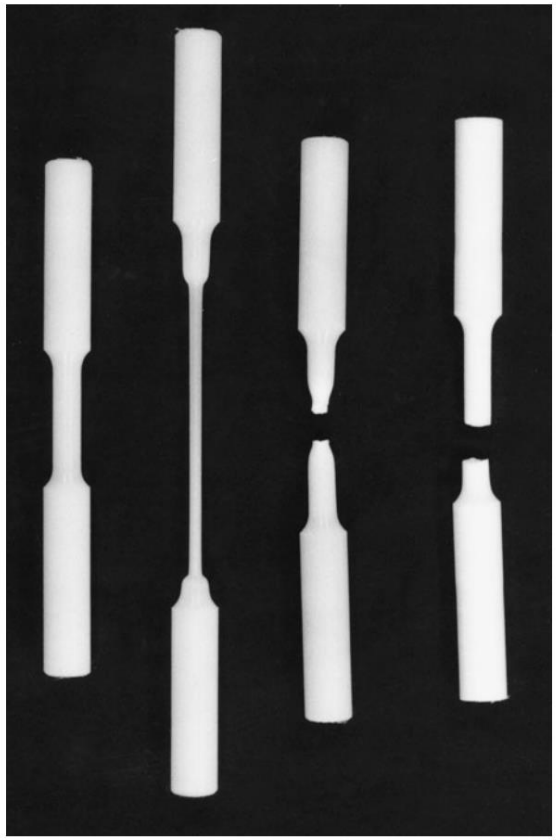

Figure 4.6 Tensile specimens of polymers (left to right): untested specimen with a 7.6 mm diameter test section, a partially tested specimen of high-density polyethylene (HDPE), and broken specimens of nylon 101 and Teflon (PTFE). (Photo by R. A. Simonds.)

Tensile Test

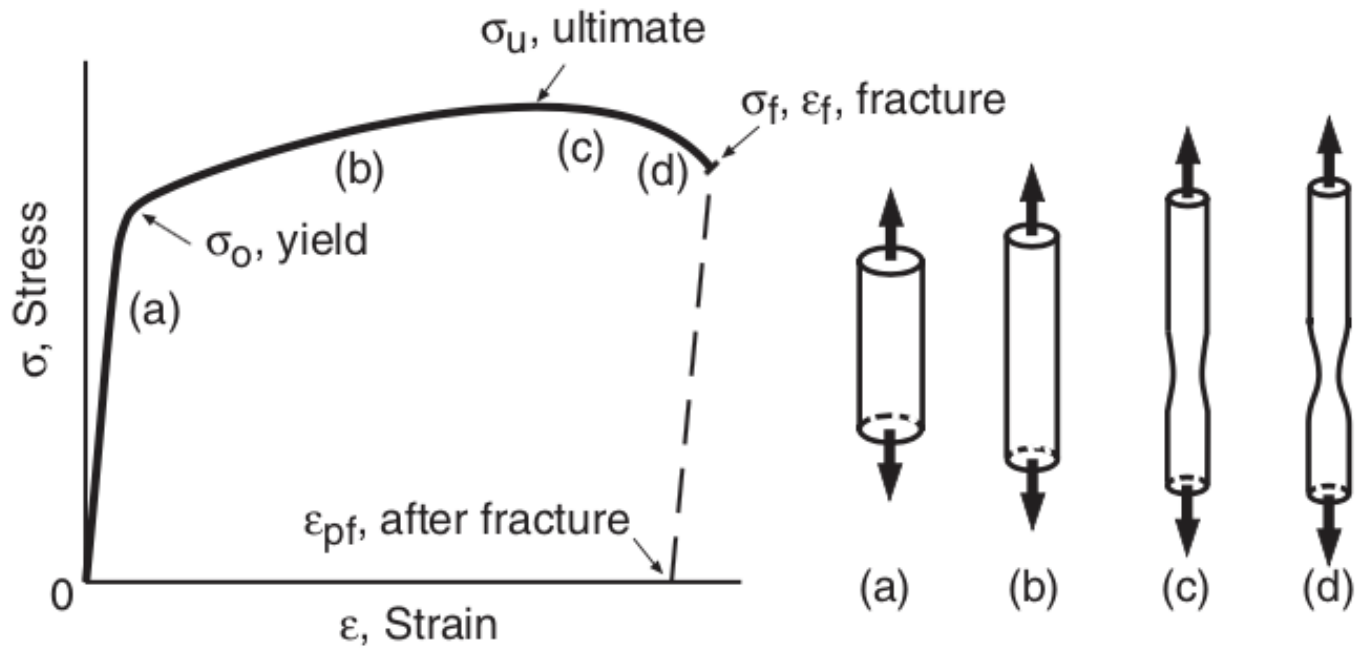

Figure 4.9 Schematic of the engineering stress–strain curve of a typical ductile metal that exhibits necking behavior. Necking begins at the ultimate stress point.

Tensile Test

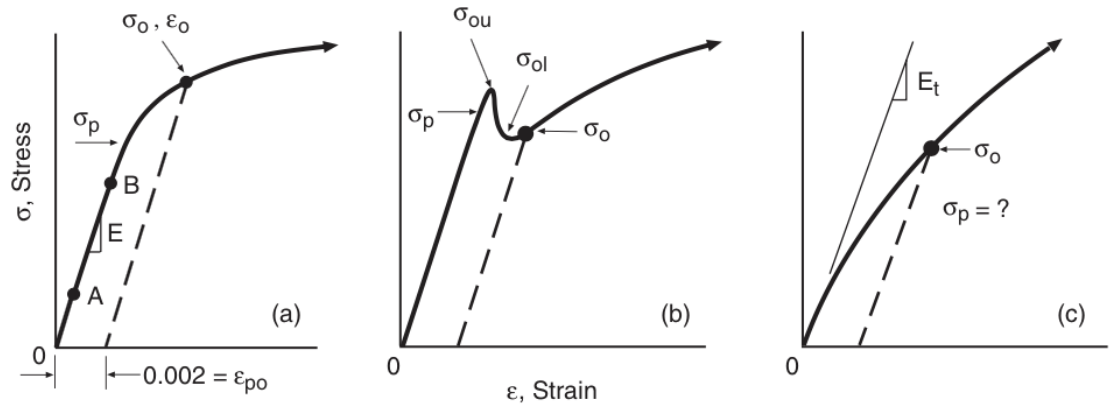

Figure 4.11 Initial portions of stress–strain curves: (a) many metals and alloys, (b) material with yield drop, and (c) material with no linear region.

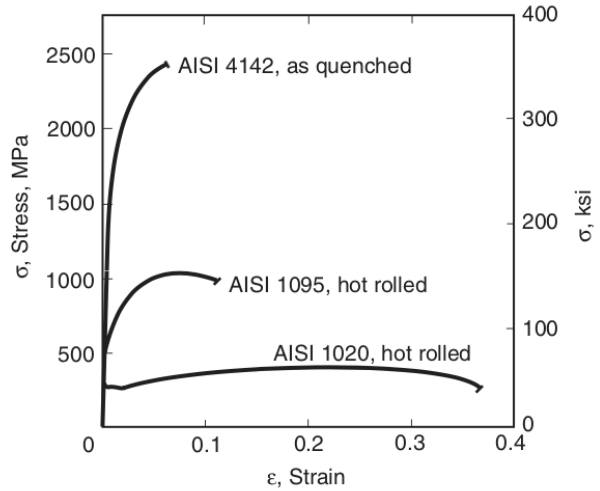

Figure 4.14 Engineering stress–strain curves from tension tests on three steels.

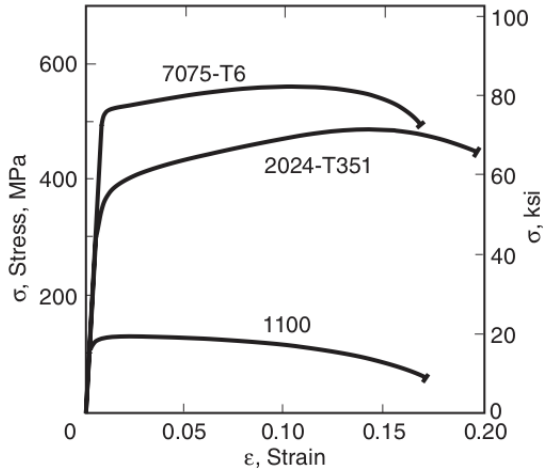

Figure 4.15 Engineering stress–strain curves from tension tests on three aluminum alloys.

Tensile Test

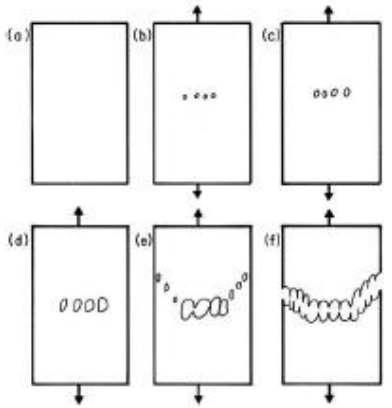

Fig. 8.14 Schematic sequence of events leading to the formation of a cup-and-cone fracture.

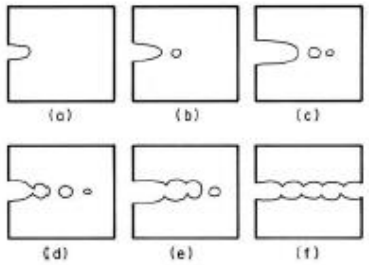

Fig. 8.15 Sequence of events in the propagation of ductile fracture by nucleation, growth, and coalescence of voids.

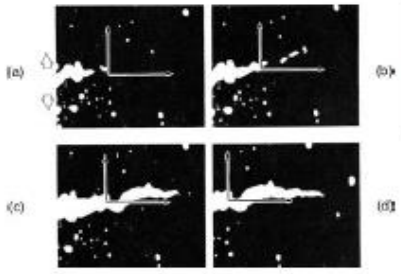

Fig. 8.16 Observation of progression of ductile fracture while specimen is stressed in high-voltage transmission electron microscope. Referential is fixed to material. (Courtesy of L. E. Murr.)

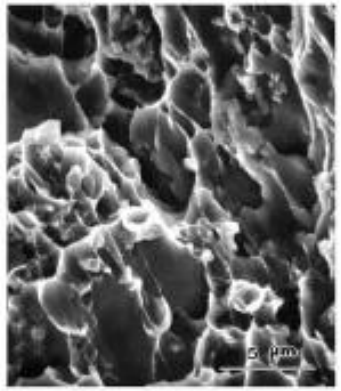

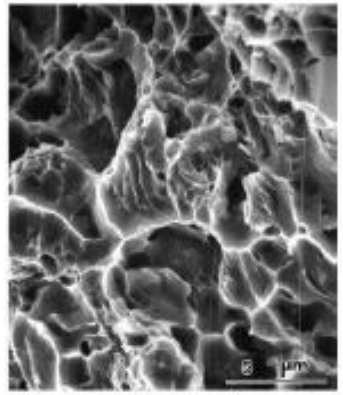

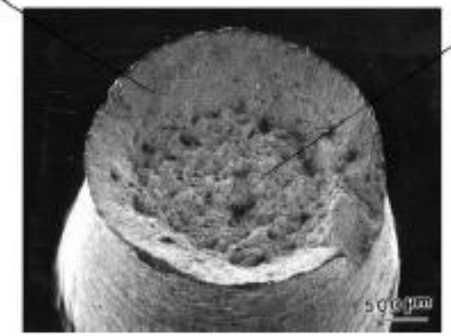

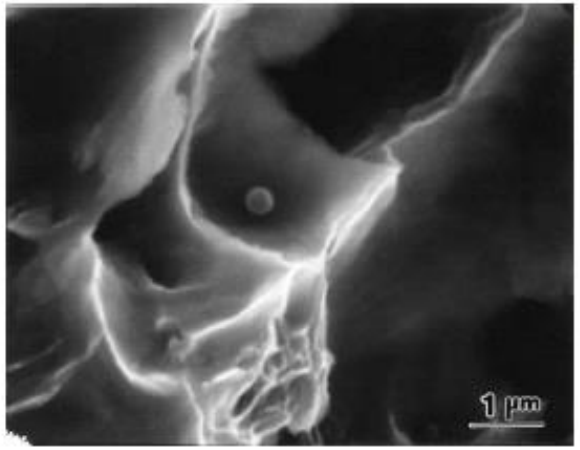

Fig. 8.12 Scanning electron micrograph of dimple fracture resulting from the nucleation, growth, and coalescence of microcavities. The micrograph shows an inclusion, which served as the microcavity nucleation site.

Tensile Test

Designation: E8/E8M – 13a

American Association State
Highway and Transportation Officials Standard
AASHTO No.: T68
An American National Standard

Standard Test Methods for Tension Testing of Metallic Materials[1]

This standard is issued under the fixed designation E8/E8M; the number immediately following the designation indicates the year of original adoption or, in the case of revision, the year of last revision. A number in parentheses indicates the year of last reapproval. A superscript epsilon (ε) indicates an editorial change since the last revision or reapproval.

This standard has been approved for use by agencies of the Department of Defense.

Impact Test

Fig. 9.1 (a) Charpy impact testing machine. (b) Charpy impact test specimen. (c) Izod impact test specimen.

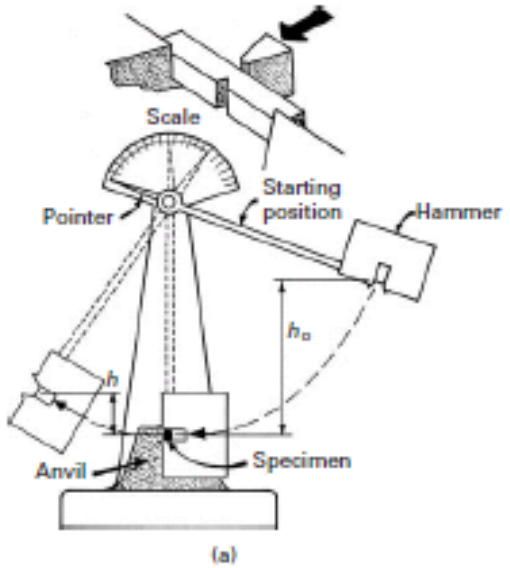

(a)

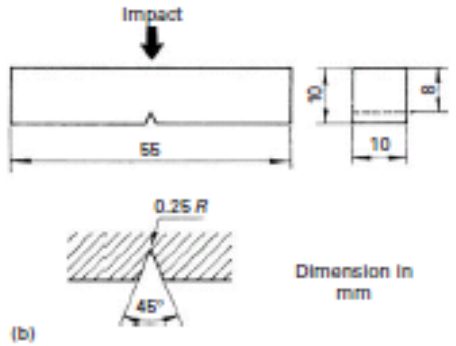

(b)

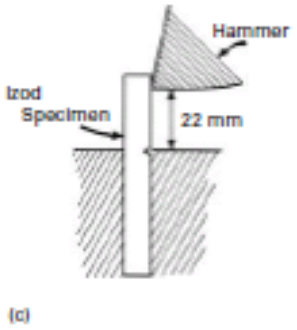

(c)

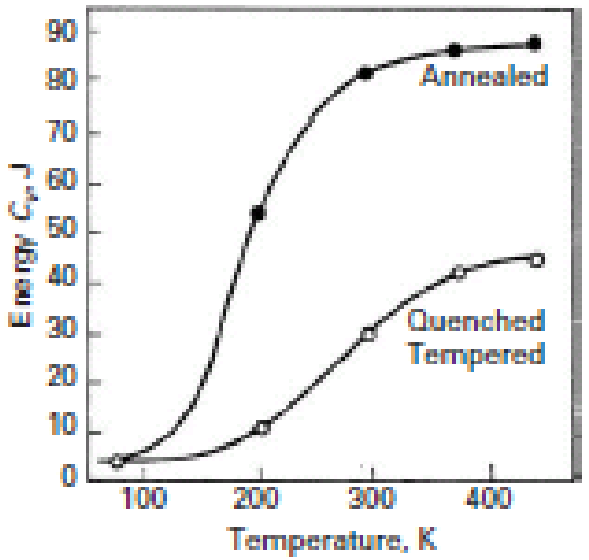

Fig. 9.2 Energy absorbed versus temperature for a steel in annealed and in quenched and tempered states. (Adapted with permission from J. C. Miguez Suarez and K. K. Chawla, *Metalurgia-ABM*, 34 (1978) 825.)

Fig. 9.3 Effect of temperature on the morphology of fracture surface of Charpy steel specimen. Test temperatures $T_a < T_b < T_c < T_d$. (a) Fully brittle fracture. (b, c) Mixed-mode fractures. (d) Fully ductile (fibrous) fracture. Each side of the specimen is 10 mm.

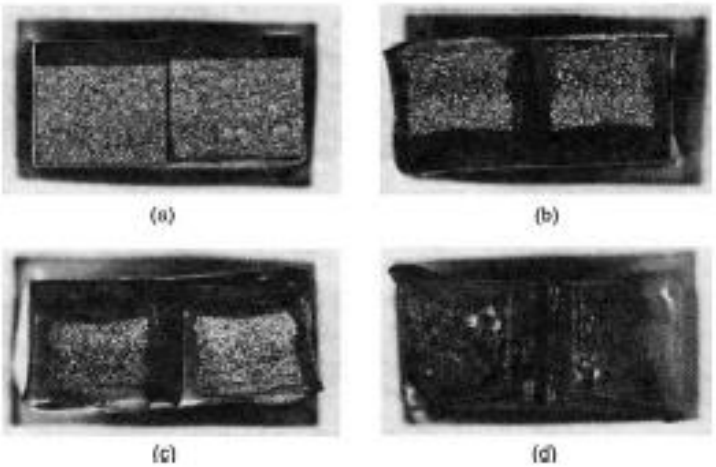

(a) (b) (c) (d)

Impact Test

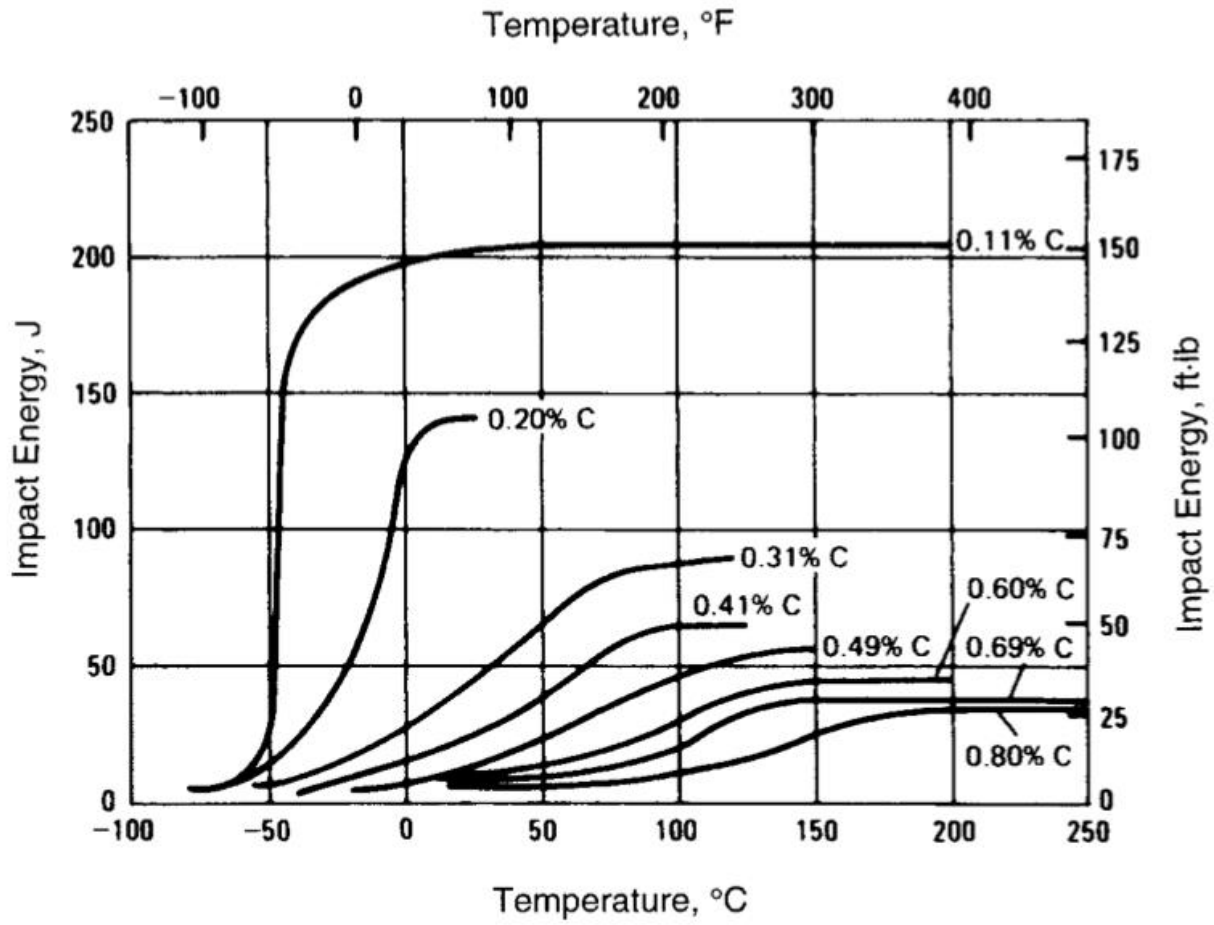

Figure 4.38 Variation in Charpy *V*-notch impact energy with temperature for normalized plain carbon steels of various carbon contents. (From [Boyer 85] p. 4.85; used with permission.)

Hardness Test

Vickers hardness

$$HV = \frac{2\,Q\,sen\frac{136}{2}}{L^2}$$

$$HV = \frac{2\,Q\,sen\frac{136}{2}}{L^2}$$

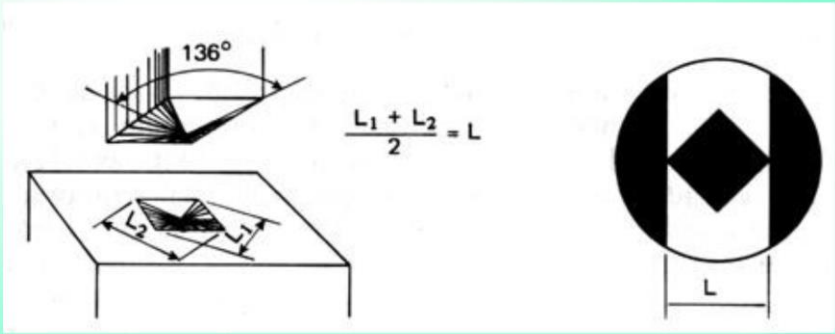

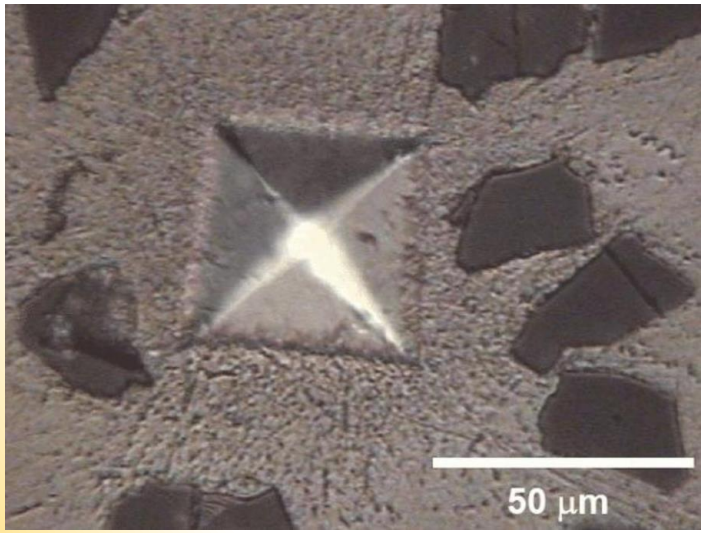

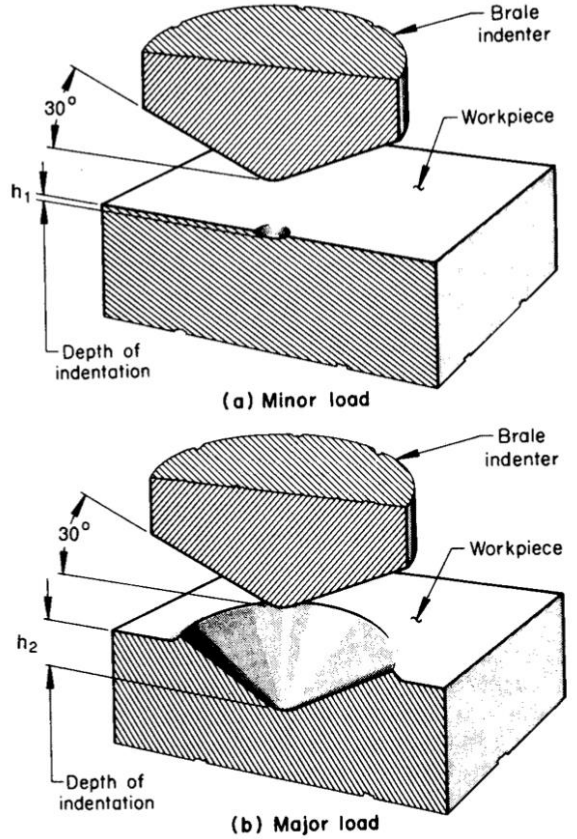

Figure 4.34 Rockwell hardness indentation made by application of (a) the minor load, and (b) the major load, on a diamond Brale indenter. (Adapted from [Boyer 85] p. 34.6; used with permission.)

Fatigue Test

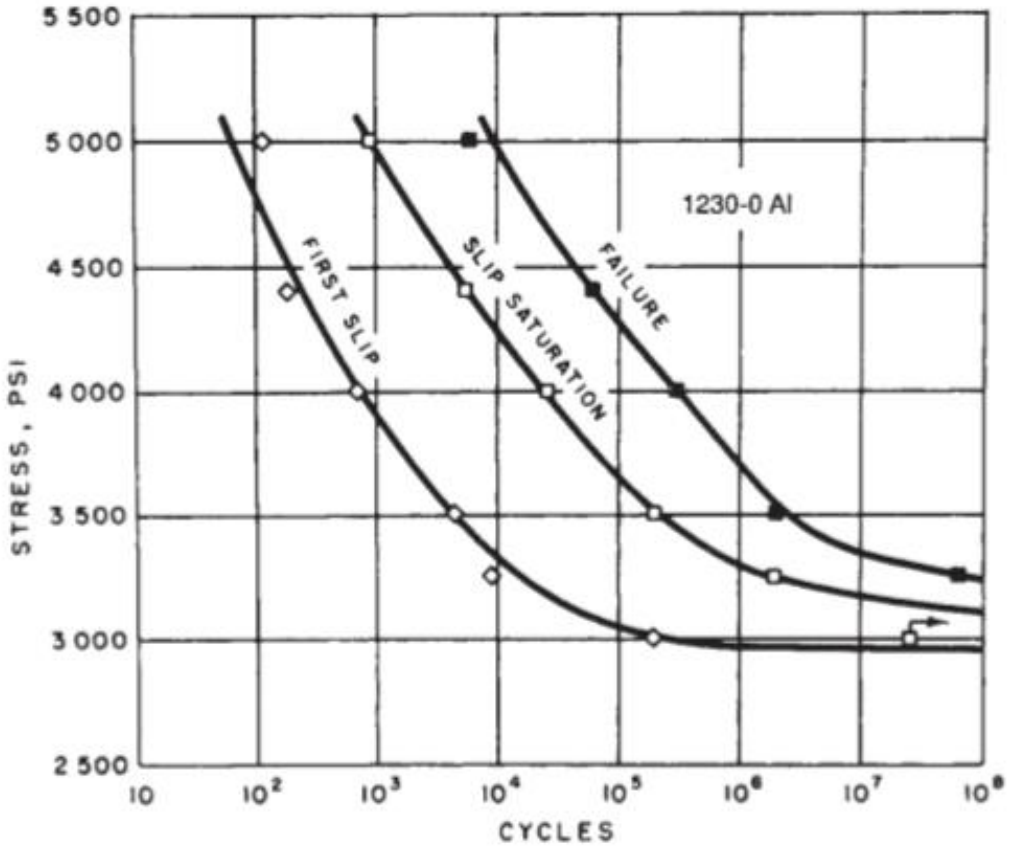

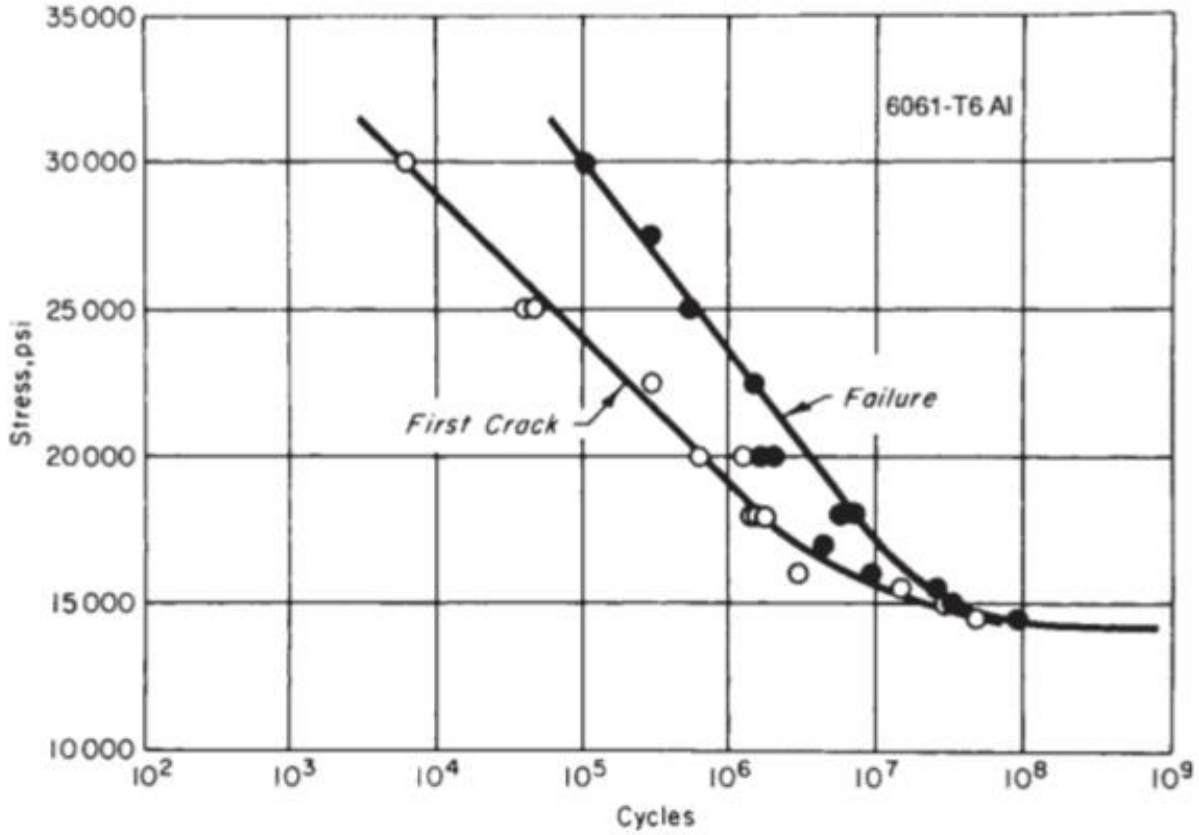

Fatigue Test

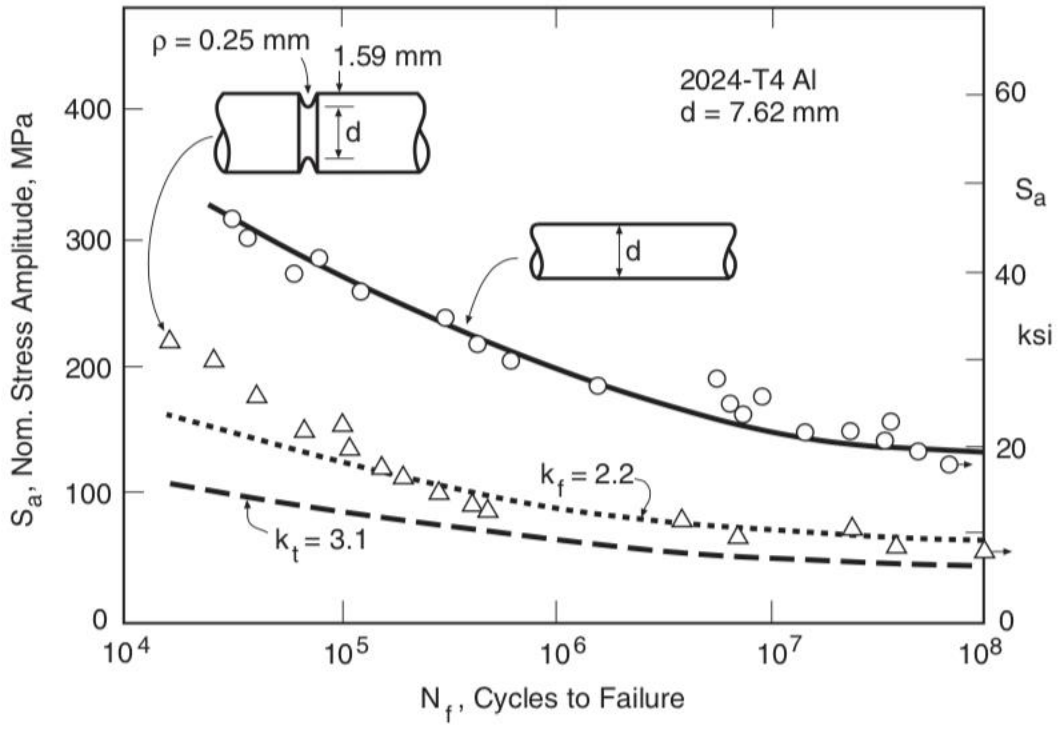

Figure 10.2 Effect of a notch on the rotating bending *S-N* behavior of an aluminum alloy, and comparisons with strength reductions using k_t and k_f. (Data from [MacGregor 52].)

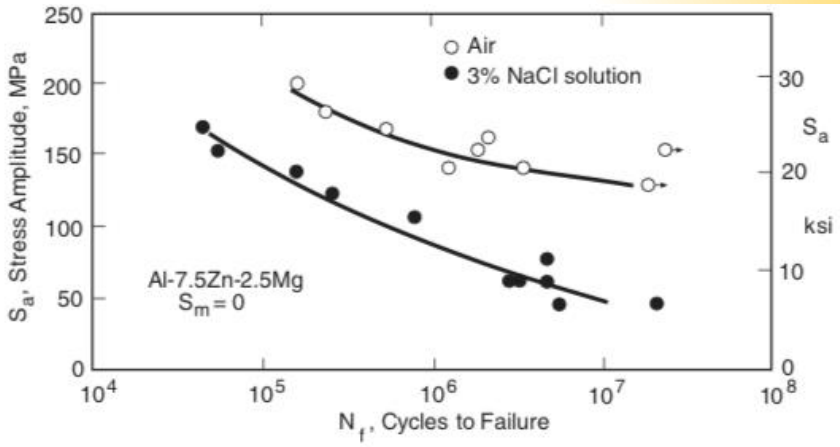

Figure 9.28 Effect of a salt solution similar to seawater on the bending fatigue behavior of an aluminum alloy. (Data from [Stubbington 61].)

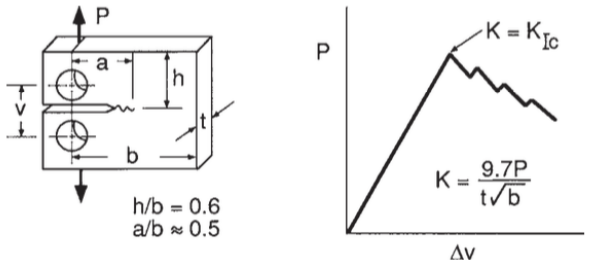

Figure 1.5 Fracture toughness test. *K* is a measure of the severity of the combination of crack size, geometry, and load. K_{Ic} is the particular value, called the *fracture toughness*, where the material fails.

Material property charts

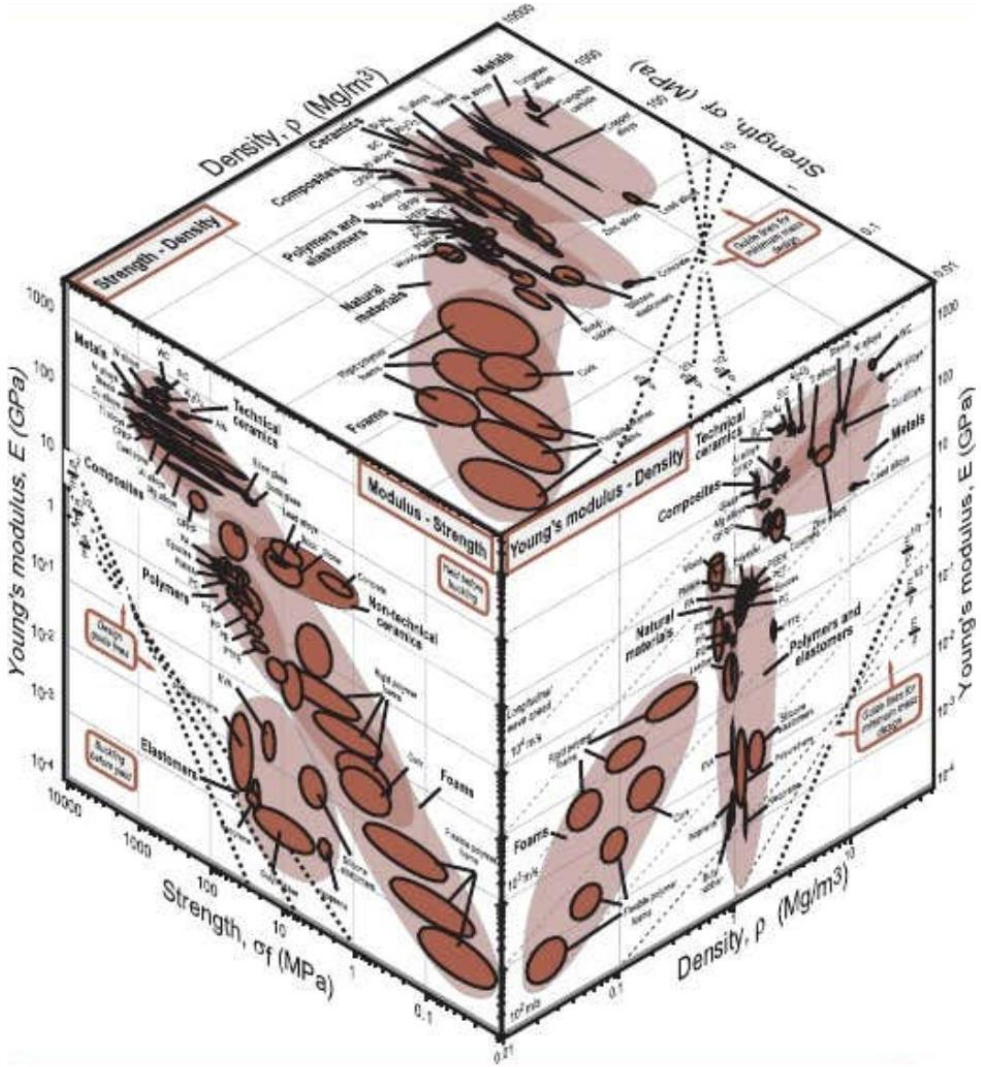

Materials Selection in Mechanical Design Third Edition- Ashby

Materials Selection in Mechanical Design Third Edition- Ashby

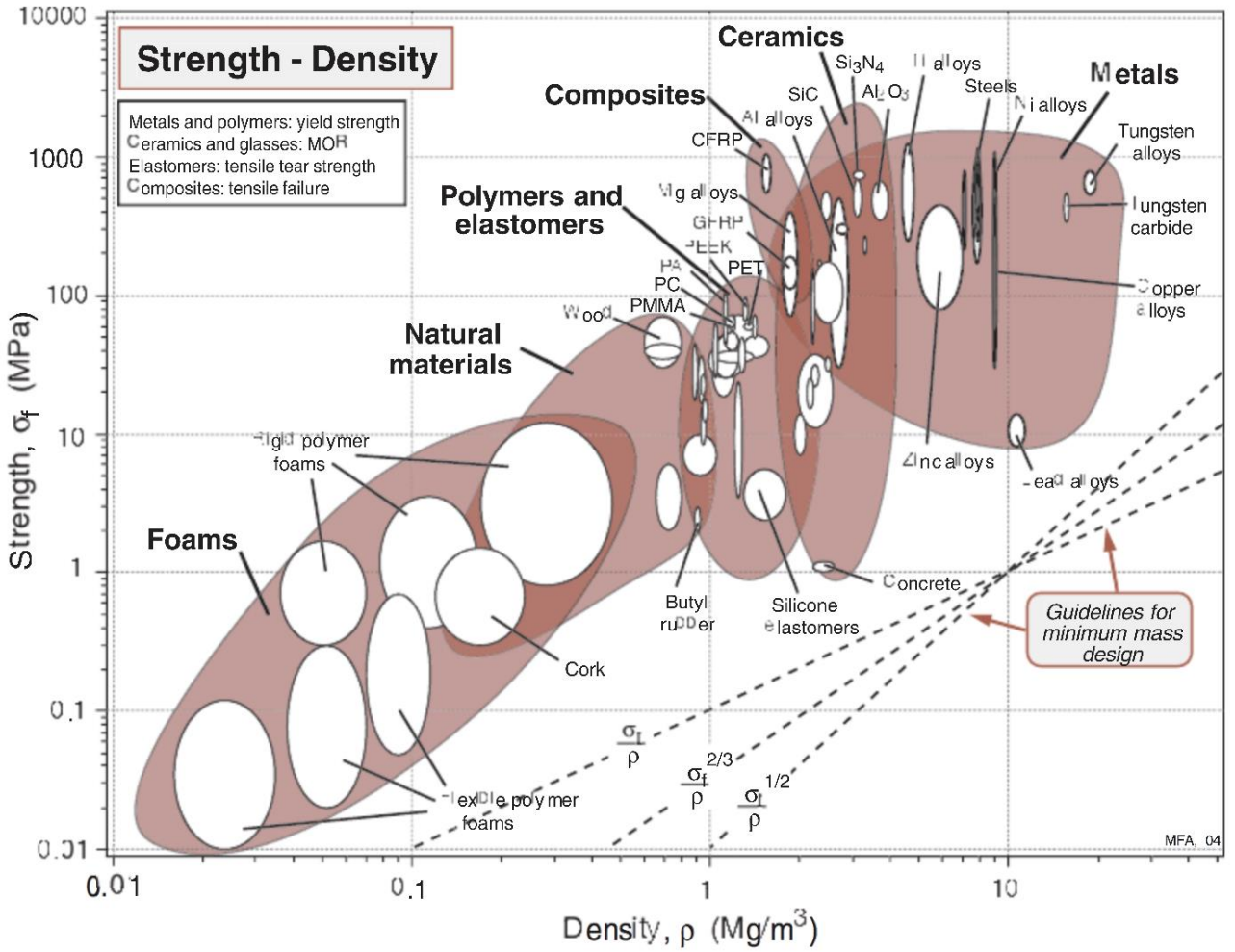

Figure 4.4 Strength, σ_f, plotted against density, ρ (yield strength for metals and polymers, compressive strength for ceramics, tear strength for elastomers and tensile strength for composites). The guidelines of constant σ_f/ρ, $\sigma_f^{2/3}/\rho$ and $\sigma_f^{1/2}/\rho$ are used in minimum weight, yield-limited, design.

Materials Design

Table 1.1 Some Major Technological Advances from 1500 A.D., the Parallel Developments in Materials and Materials Testing, and Failures Related to Behavior of Materials

Years	Technological Advance	New Materials Introduced	Materials Testing Advances	Failures
1500's 1600's	Dikes Canals Pumps Telescope	(Stone, brick, wood, copper, bronze, and cast and wrought iron in use)	Tension (L. da Vinci) Tension, bending (Galileo) Pressure burst (Mariotte) Elasticity (Hooke)	
1700's	Steam engine Cast iron bridge	Malleable cast iron	Shear, torsion (Coulomb)	
1800's	Railroad industry Suspension bridge Internal combustion engine	Portland cement Vulcanized rubber Bessemer steel	Fatigue (Wöhler) Plasticity (Tresca) Universal testing machines	Steam boilers Railroad axles Iron bridges
1900's 1910's	Electric power Powered flight Vacuum tube	Alloy steels Aluminum alloys Synthetic plastics	Hardness (Brinell) Impact (Izod, Charpy) Creep (Andrade)	Quebec bridge Boston molasses tank
1920's 1930's	Gas-turbine engine Strain gage	Stainless steel Tungsten carbide	Fracture (Griffith)	Railroad wheels, rails Automotive parts
1940's 1950's	Controlled fission Jet aircraft Transistor; computer Sputnik	Ni-base alloys Ti-base alloys Fiberglass	Electronic testing machine Low-cycle fatigue (Coffin, Manson) Fracture mechanics (Irwin)	Liberty ships Comet airliner Turbine generators
1960's 1970's	Laser Microprocessor Moon landing	HSLA steels High-performance composites	Closed-loop testing machine Fatigue crack growth (Paris) Computer control	F-111 aircraft DC-10 aircraft Highway bridges
1980's 1990's	Space station Magnetic levitation	Tough ceramics Al-Li alloys	Multiaxial testing Direct digital control	Alex. Kielland rig Surgical implants
2000's 2010's	Sustainable energy Extreme fossil fuel extraction	Nanomaterials Bio-inspired materials	User-friendly test software	Space Shuttle tiles Deepwater Horizon offshore oil rig

Source: [Herring 89], [Landgraf 80], [Timoshenko 83], [Whyte 75], *Encyclopedia Britannica*, news reports.

Size Scales

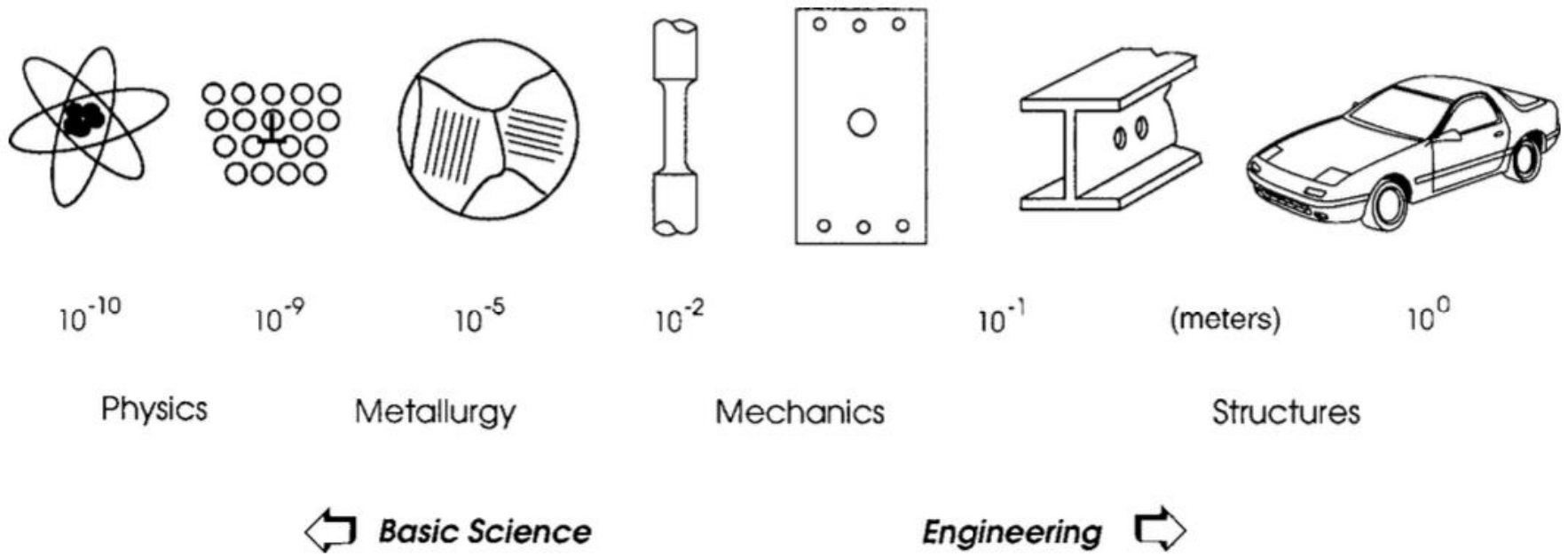

Figure 2.2 Size scales and disciplines involved in the study and use of engineering materials. (Illustration courtesy of R. W. Landgraf, Howell, MI.)

Size Scales:

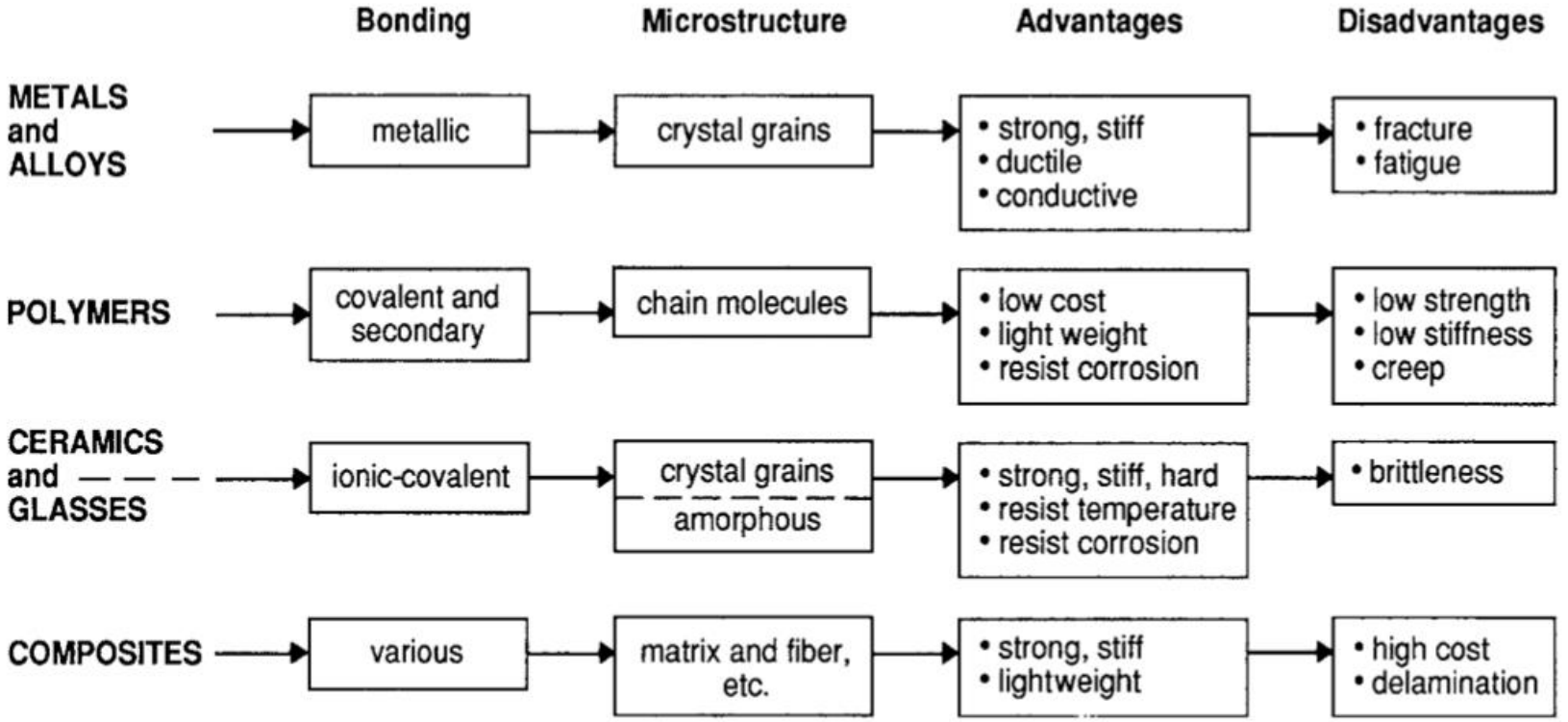

Figure 2.1 General characteristics of the major classes of engineering materials.

Microstructure

There exist 6 structural levels of matter down to the final elementary particles (Fig. 1) . Microstructure is the Material Science is concerned with the relation be- term used here for the level between phases (crystals
tween structure and macroscopic properties. There and glasses) and macroscopic structures.

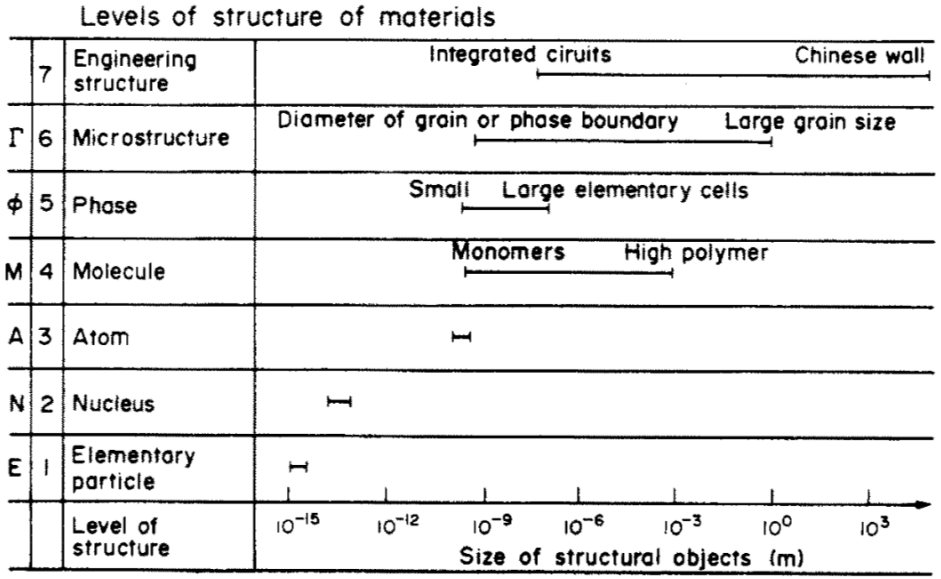

Fig. 1. Seven levels of structure.

Atom is (Physics) the smallest component of an element having the chemical properties of the element, consisting of a nucleus containing combinations of neutrons and protons and one or more electrons bound to the nucleus by electrical attraction; the number of protons determines the identity of the element.

A **molecule** is an electrically neutral group of two or more atoms held together by chemical bonds. Molecules are distinguished from ions by their lack of electrical charge.

Acta metall Vol. 32, No. 5. pp. 615-627, 1984
E. HORNBOGEN - ON THE MICROSTRUCTURE OF ALLOYS

Microstructure

"The term microstructure is still often reserved to objects which are visible by the methods of light microscopy. Its quantitative description has achieved a high degree of perfection. Advances of electron microscopy (TEM, SEM) and more recently field ion microscopy (FIM), however, have expanded our horizon so that it seems on time to extend the definition of microstructure. and to realise that its importance is comparable to that of other levels of structure "

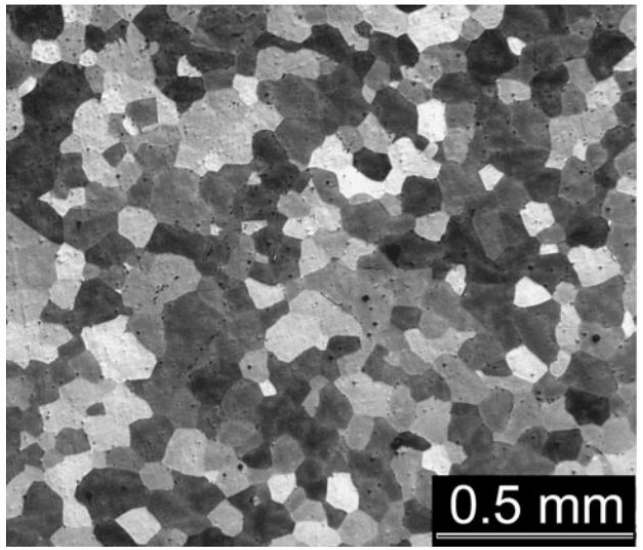

Figure 2.12 Crystal grain structure in a magnesium alloy containing 12 wt% lithium. This cast metal was prepared in a high-frequency induction melting furnace under an argon atmosphere. (Photo courtesy of Milo Kral, University of Canterbury, Christchurch, New Zealand; used with permission.)

Acta metall Vol. 32, No. 5. pp. 615-627, 1984
E. HORNBOGEN - ON THE MICROSTRUCTURE OF ALLOYS

Mechanical Behavior and Microstructural Features

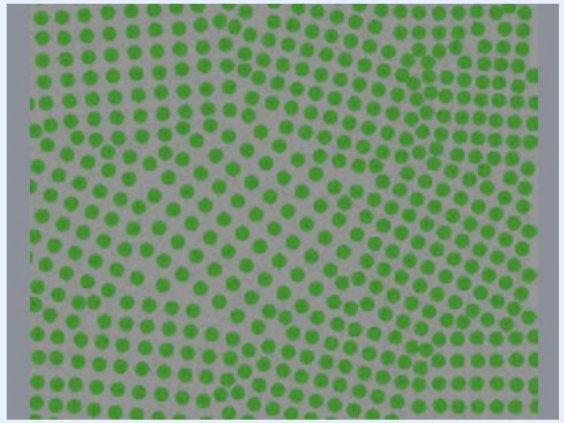

Grain boundary - Wikipedia
en.wikipedia.org

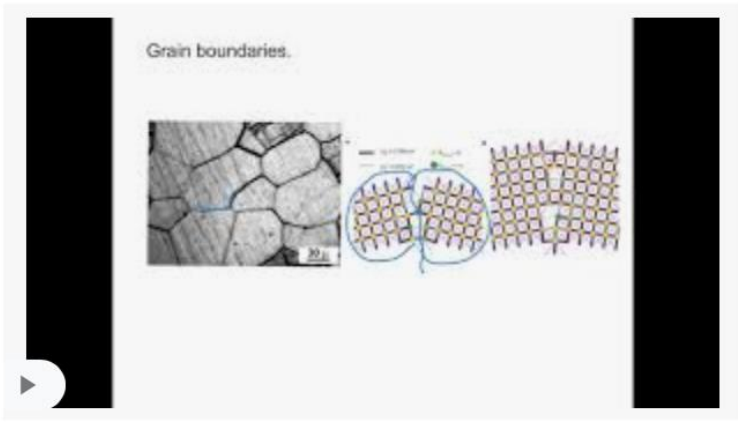

Grain boundaries - YouTube
youtube.com

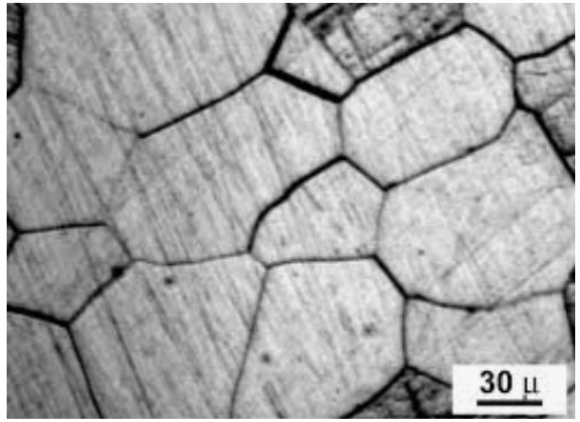

Grain boundary - Wikipedia
en.wikipedia.org

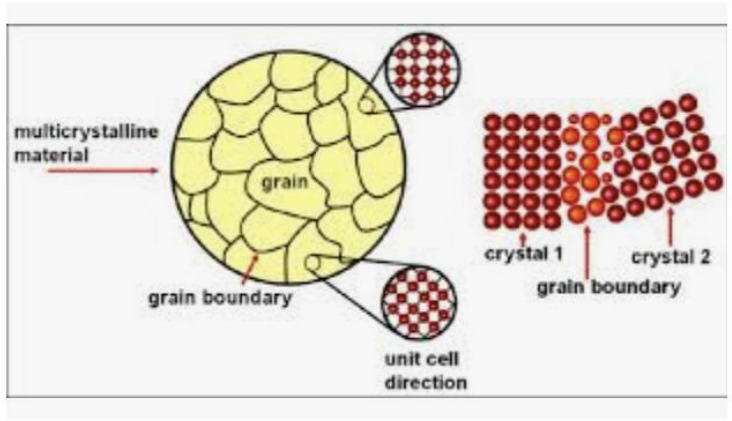

1: Grains and grain boundaries in a ...
researchgate.net

Mechanical Behavior and Microstructural Features

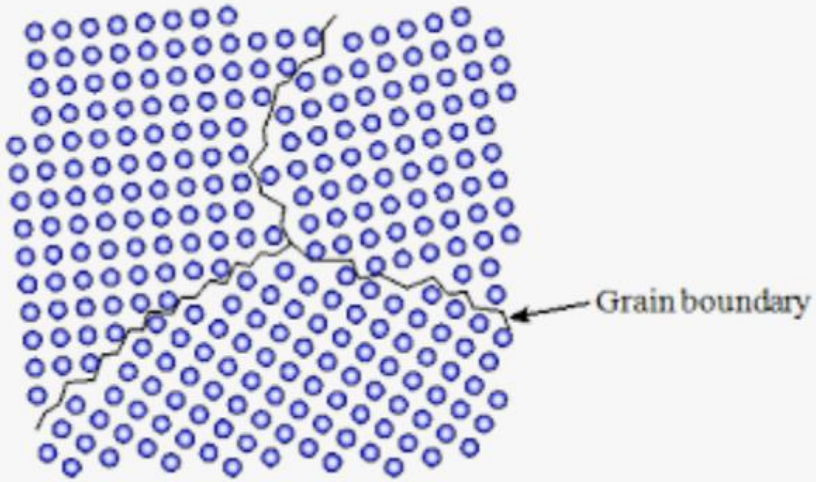

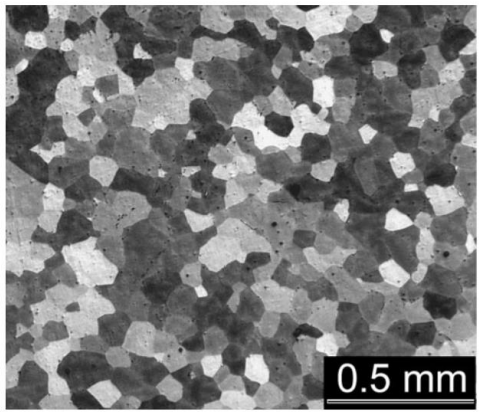

Figure 2.12 Crystal grain structure in a magnesium alloy containing 12 wt% lithium. This cast metal was prepared in a high-frequency induction melting furnace under an argon atmosphere. (Photo courtesy of Milo Kral, University of Canterbury, Christchurch, New Zealand; used with permission.)

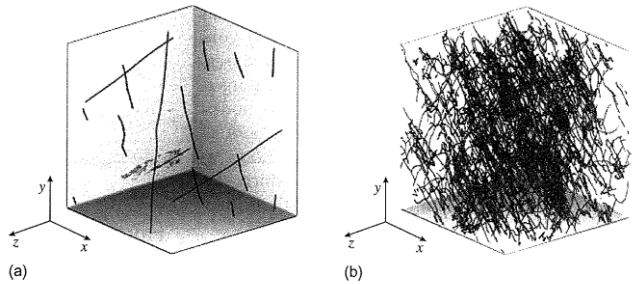

FIGURE 2.20
(a) Initial dislocation arrangement for the DD simulation of a molybdenum single crystal under applied uniaxial strain. (b) Dislocation microstructure when the strain reaches 0.3%. *(From Bulatov and Cai (2006),* Computer Simulations of Dislocations, *Oxford University Press. With permission from Oxford University Press (www.oup.co.uk).*

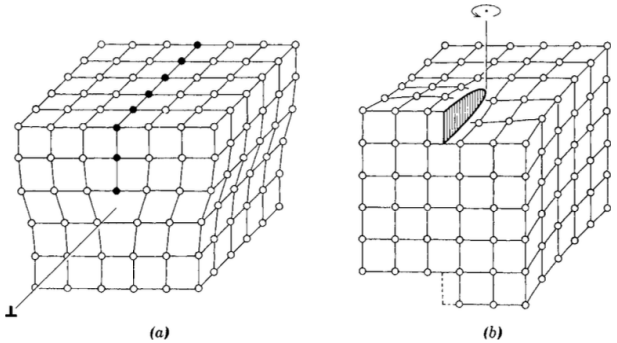

Figure 2.14 The two basic types of dislocations: (a) edge dislocation, and (b) screw dislocation. (From [Hayden 65] p. 63; used with permission.)

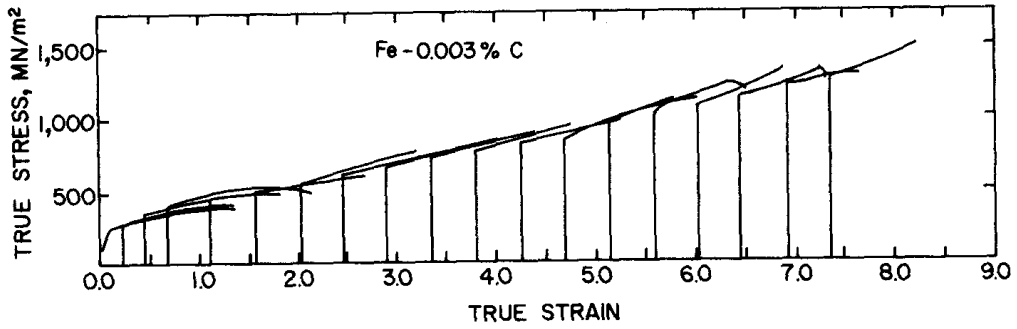

Figure 3.11 Stress–strain curves for Fe–0.003% C alloy wire, deformed to increasing strains by drawing; each curve is started at the strain corresponding to the prior wire-drawing reduction. (Courtesy of H. J. Rack)

Mechanical Behavior and Microstructural Features

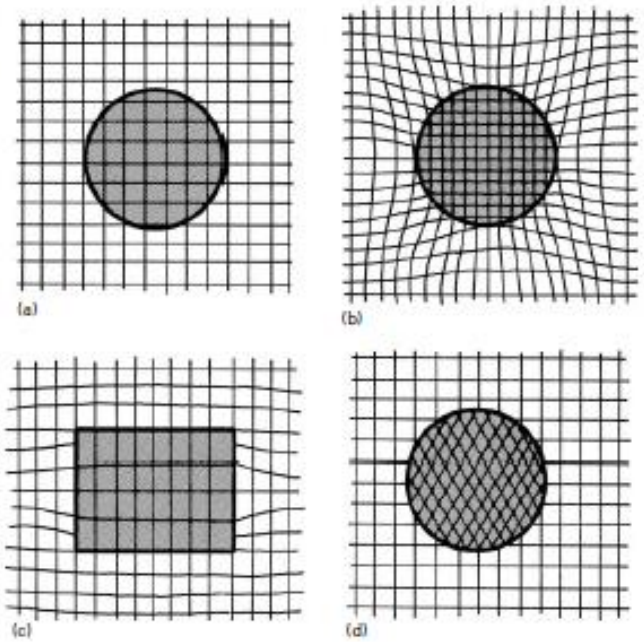

Fig. 10.15 Different crystallographic relationships between matrix and second phase. (a) Complete coherency. (b) Coherency with strained, but continuous, lattice planes across the boundary. (c) Semicoherent, partial continuity of lattice planes across the interface. (d) Incoherent equilibrium precipitate, θ; no continuity of lattice planes across the interface.

Fig. 10.16 Interfacial dislocations formed in a semicoherent precipitate. (From G. C. Weatherly and R. B. Nicholson, *Phil. Mag.*, 17 (1968), 801.)

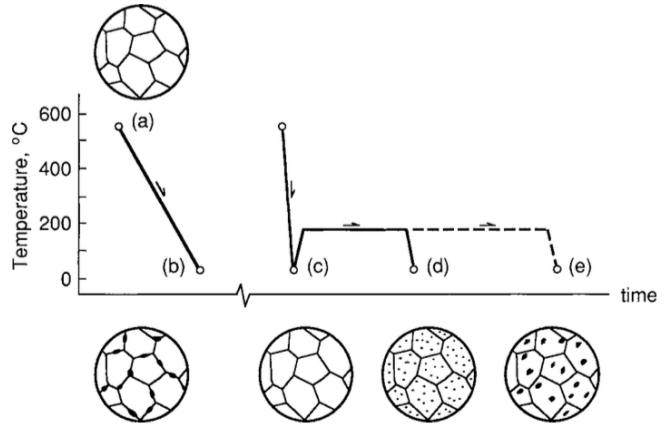

Figure 3.4 Precipitation hardening of aluminum alloyed with 4% Cu. Slow cooling from a solid solution (a) produces grain boundary precipitates (b). Rapid cooling to obtain a supersaturated solution (c) can be followed by aging at a moderate temperature to obtain fine precipitates within grains (d), but overaging gives coarse precipitates (e).

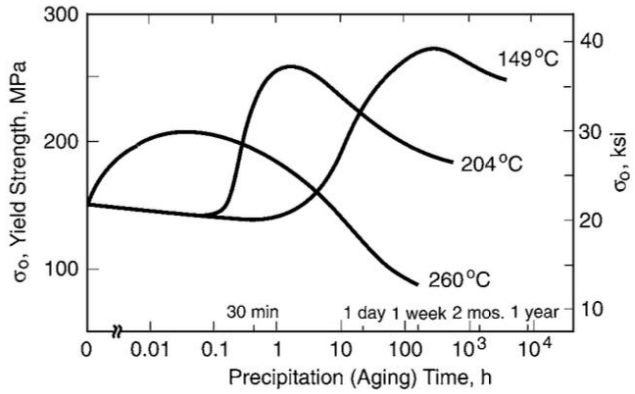

Figure 3.5 Effects of precipitation (aging) time and temperature on the resulting yield strength in aluminum alloy 6061. (Adapted from [Boyer 85] p. 6.7; used with permission.)

Mechanical Behavior and Microstructural Features

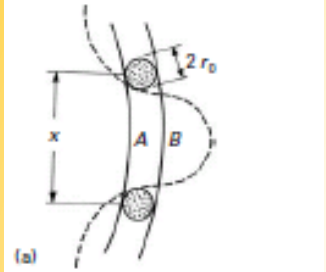

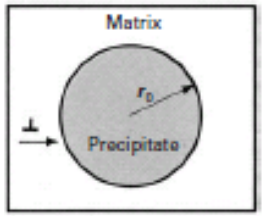

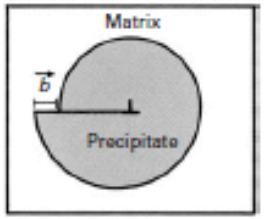

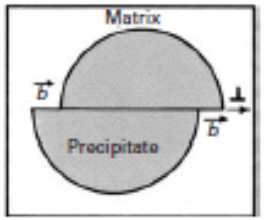

Fig. 10.21 (a) Dislocation at two successive positions A and B. (b) Dislocation shearing precipitate.

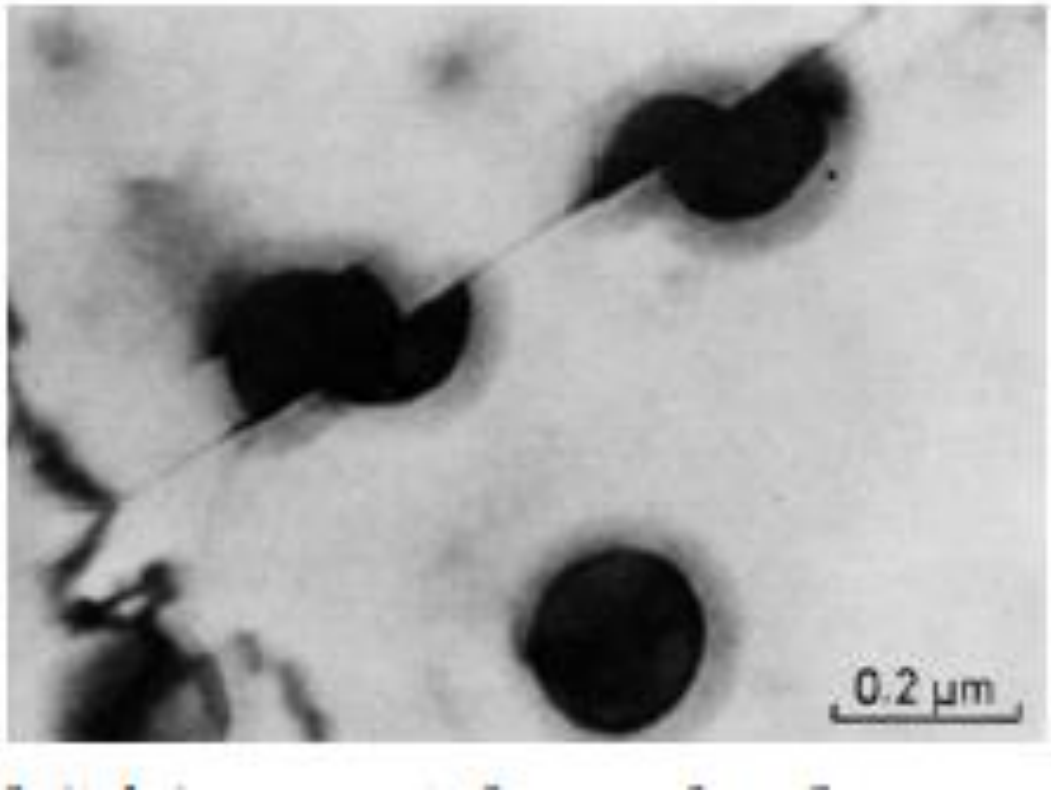

Fig. 10.20 γ'-precipitate particles sheared by dislocations in a Ni–19% Cr–6% Al alloy aged at 750 °C for 540 hours and strained 2%. The arrows indicate the two slip-plane traces (transmission electron microscopy) (Courtesy of H. Gleiter.)

Mechanical Behavior and Microstructural Features

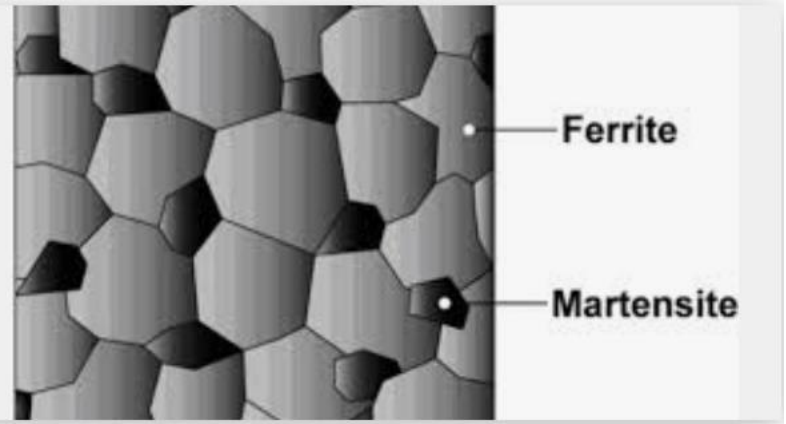

nique characteristics of dual-phase steels
efabricator.com

The

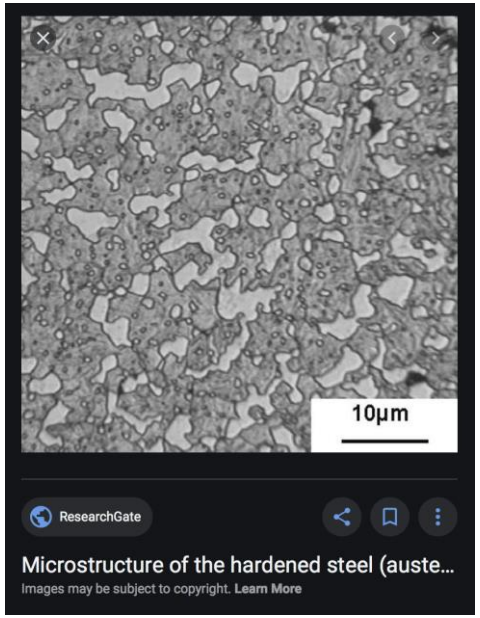

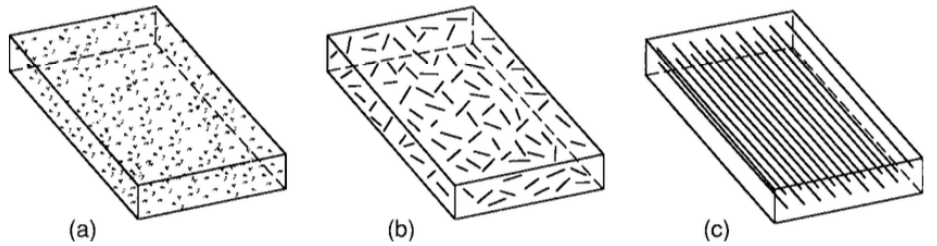

Figure 3.23 Composites reinforced by (a) particles, (b) chopped fibers or whiskers, and (c) continuous fibers. (Adapted from [Budinski 96] p. 121; © 1996 by Prentice Hall, Upper Saddle River, NJ; reprinted with permission.)

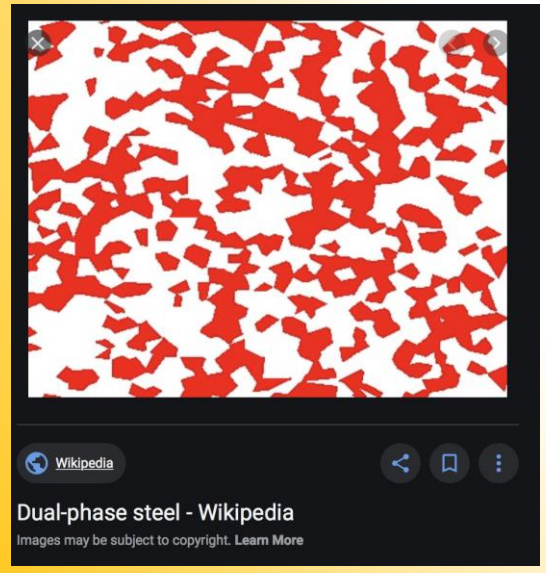

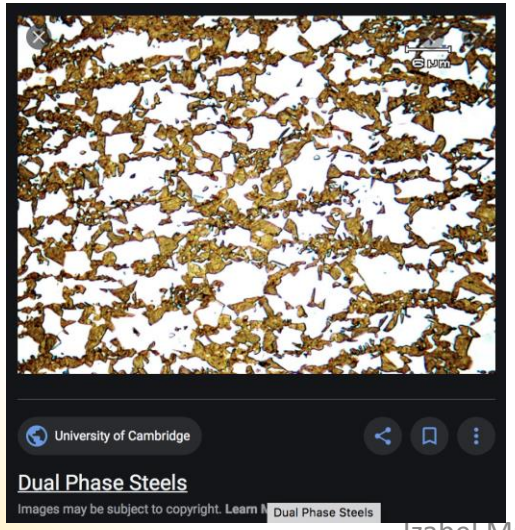

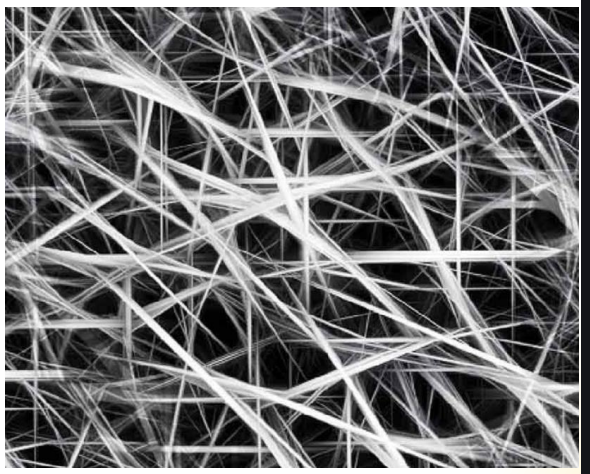

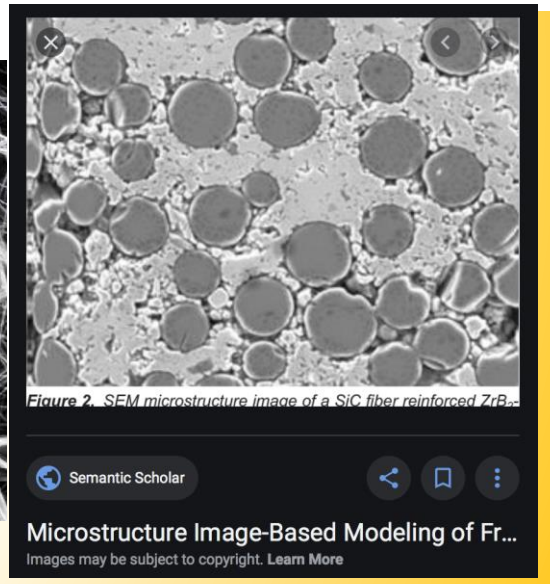

Microstructure's Features

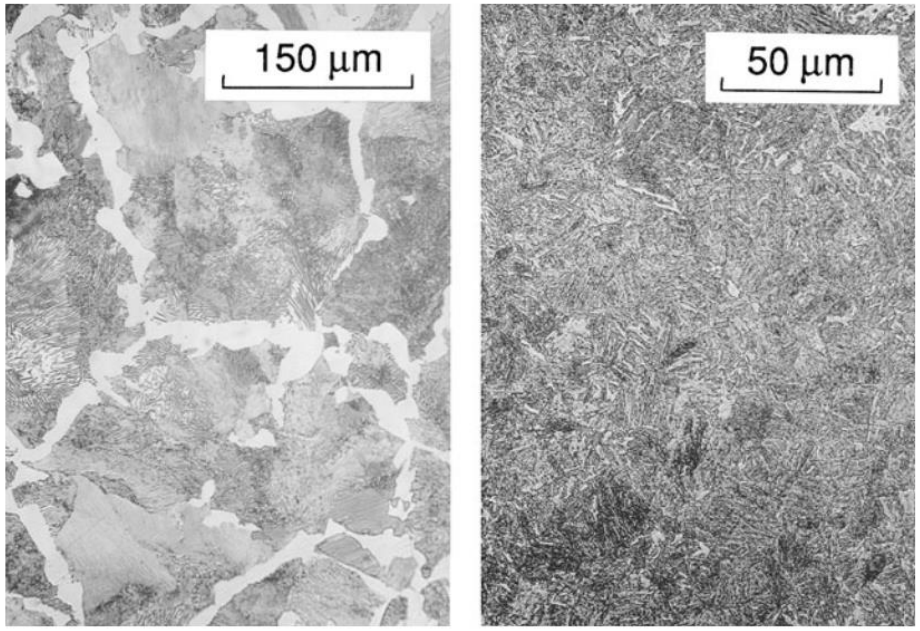

Figure 3.8 Steel microstructures: ferrite-pearlite structure in normalized AISI 1045 steel (left), with ferrite being the light-colored areas, and pearlite the striated regions; quenched and tempered structure in AISI 4340 steel (right). (Left photo courtesy of Deere and Co., Moline, IL.)

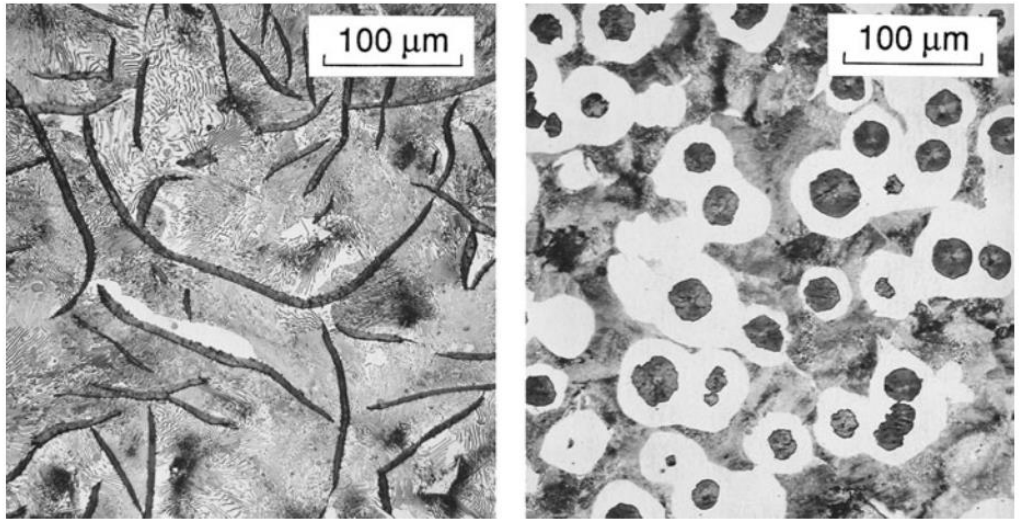

Figure 3.7 Microstructures of gray cast iron (left) and ductile (nodular) cast iron (right). The graphite flakes on the left are the heavy dark bands, and the graphite nodules on the right are the dark shapes. In gray iron (left), the fine lines are a pearlitic structure similar to that in mild steel. (Photos courtesy of Deere and Co., Moline, IL.)

Microstructure's Features

Microstructure's Features

Microstructure's Features

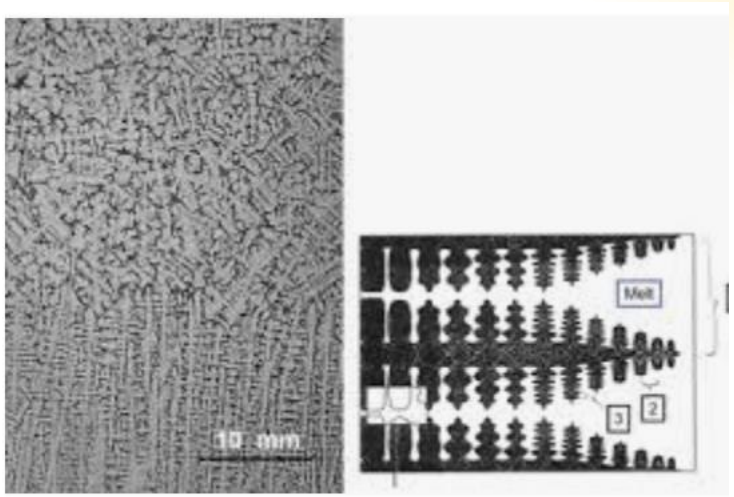

Columnar Dendrite - an overview ...
sciencedirect.com

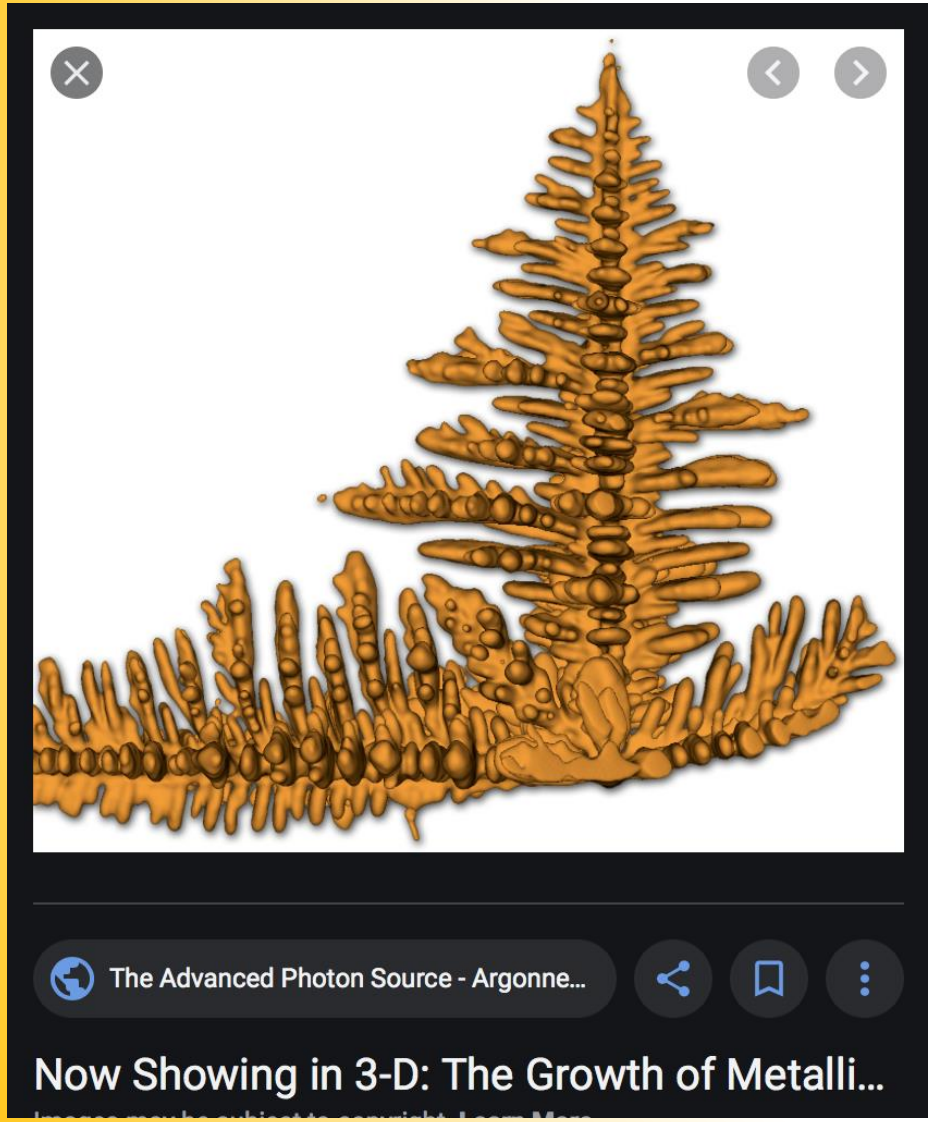

Microstructure's Features

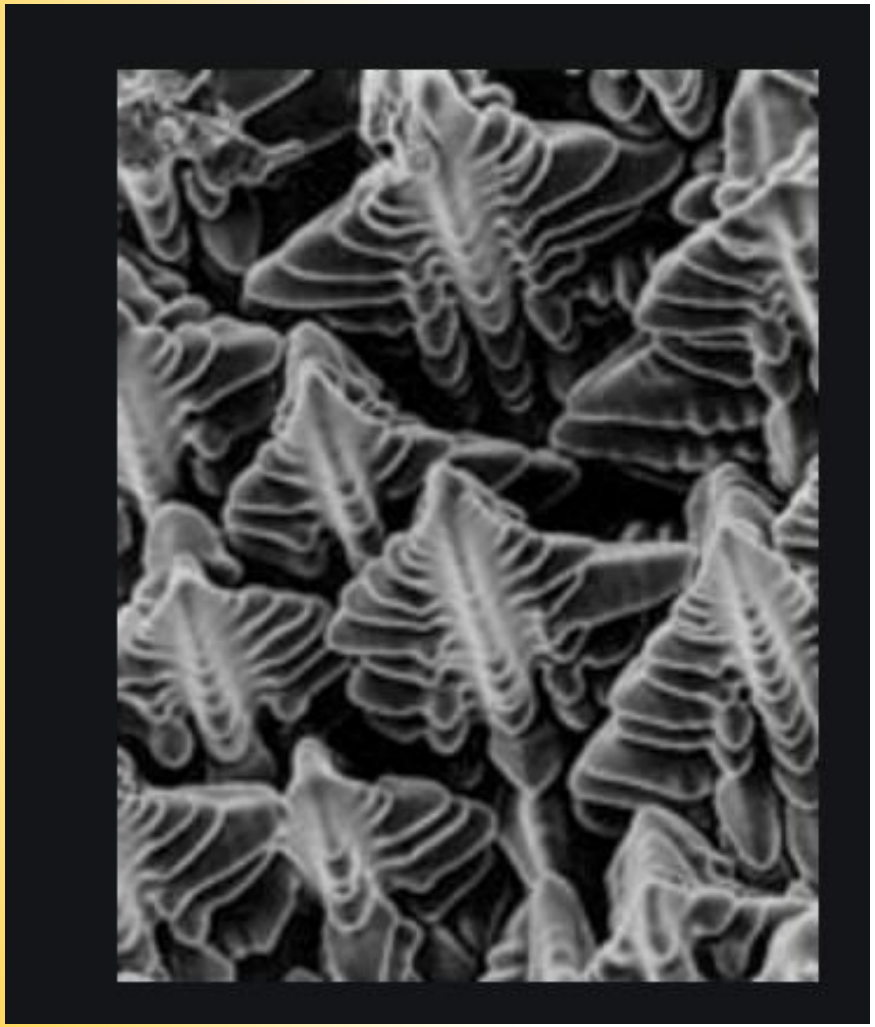

Phase Diagram

Fe-C System

Thermodynamics

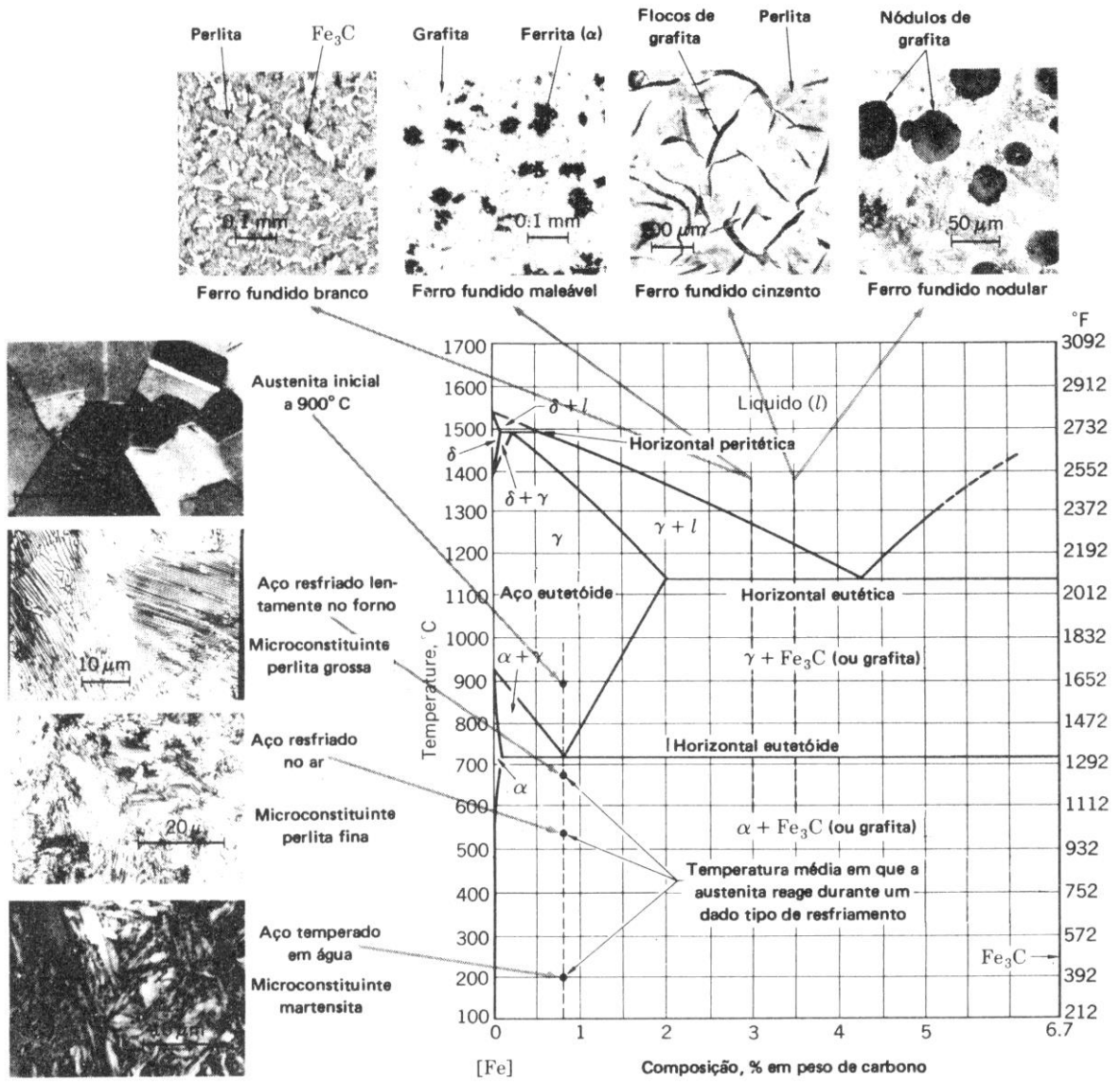

TTT and CRC diagrams

Kinetics

Fe-C System

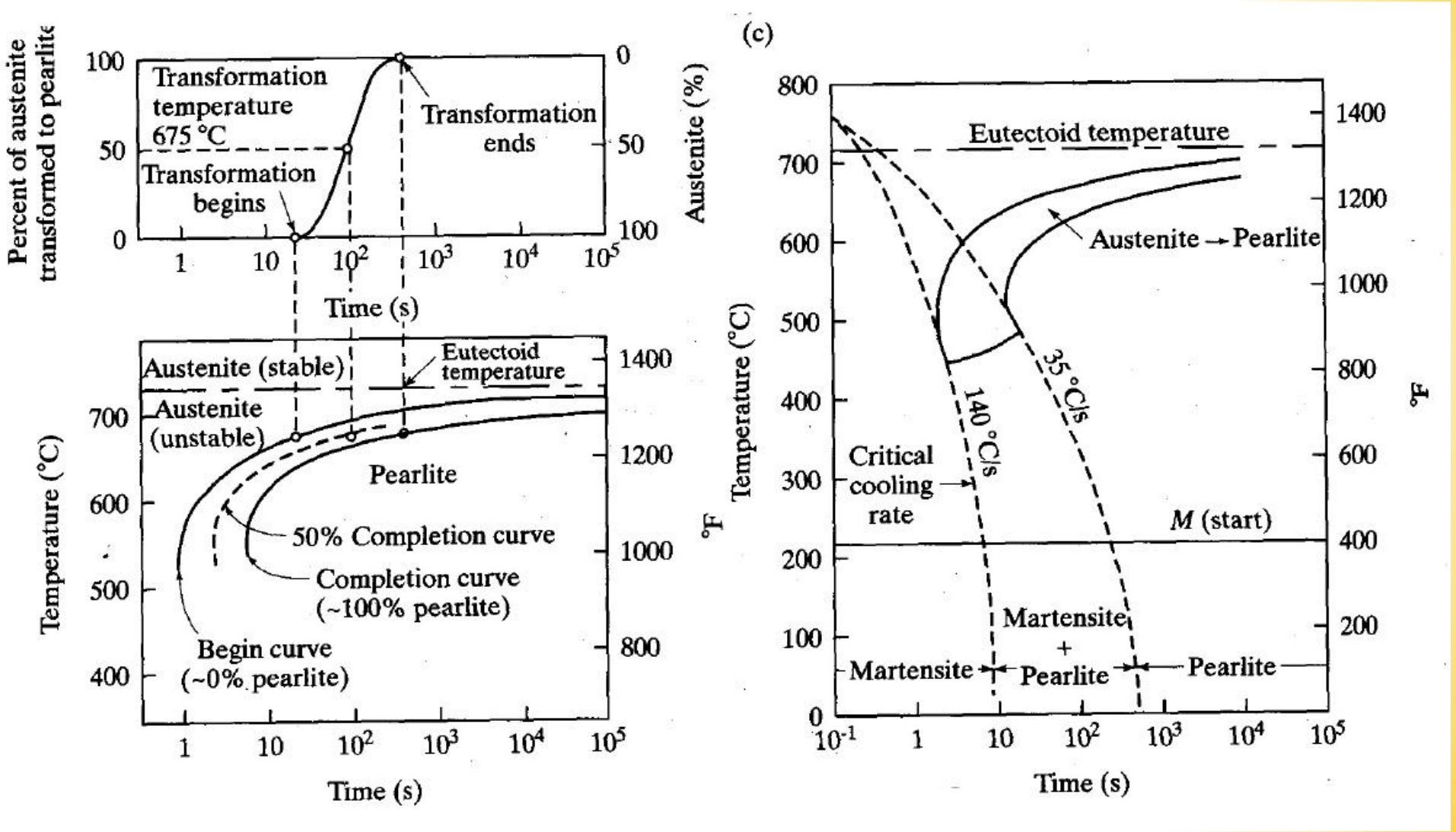

Fe-C System

Kinetics

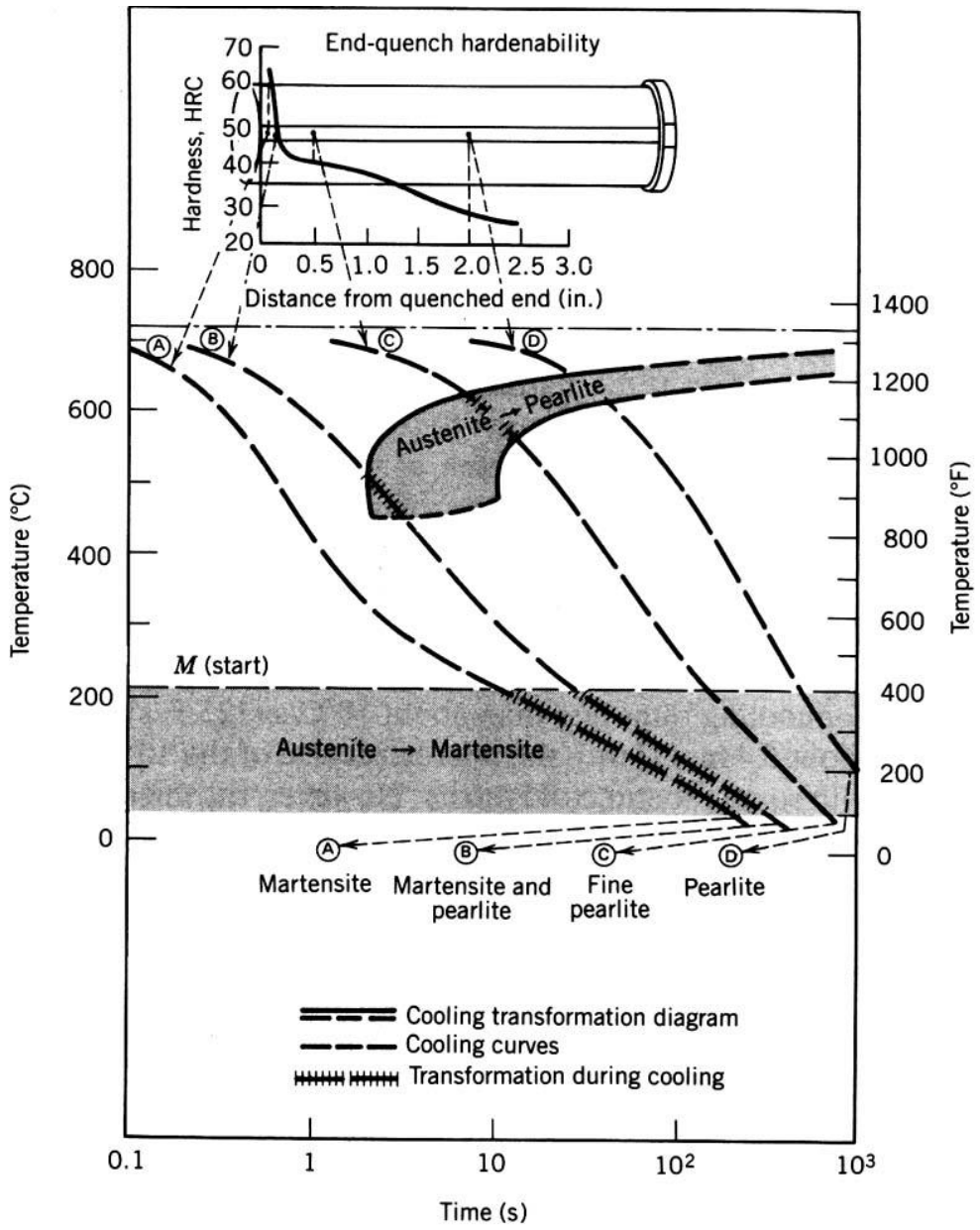

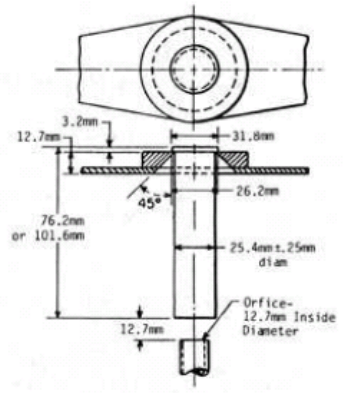

Figura 6. Esquema do dispositivo para realização do ensaio Jominy.

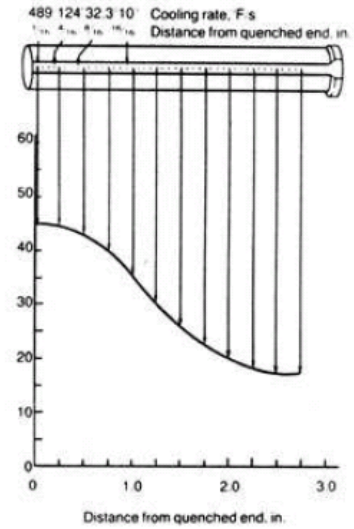

Figura 7. Medidas de dureza ao longo do corpo de prova.

Os resultados do ensaio permitem comparar a temperabilidade de diferentes aços e também servem como uma maneira de avaliar o material recebido (controle de qualidade).

Fe-C System

Kinetics
Stable and Metastable phases

Composição química (porcentagem em peso) **Aço 1045**

C	Mn	P, max	S, max	Si	Ni	Cr	Mo	Outros elementos
0,43-0,50	0,60-0,90	0,040	0,050	-	-	-	-	-

Normalizado

Temperado

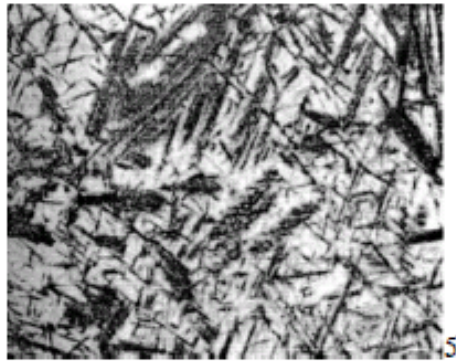

Composição química (porcentagem em peso) **Aço 4140**

C	Mn	P, max	S, max	Si	Ni	Cr	Mo	Outros elementos
0,38-0,43	0,75-1,00	0,035	0,040	0,20-0,35	-	0,80-1,10	0,15-0,25	-

Normalizado

Temperado

Mechanical behavior

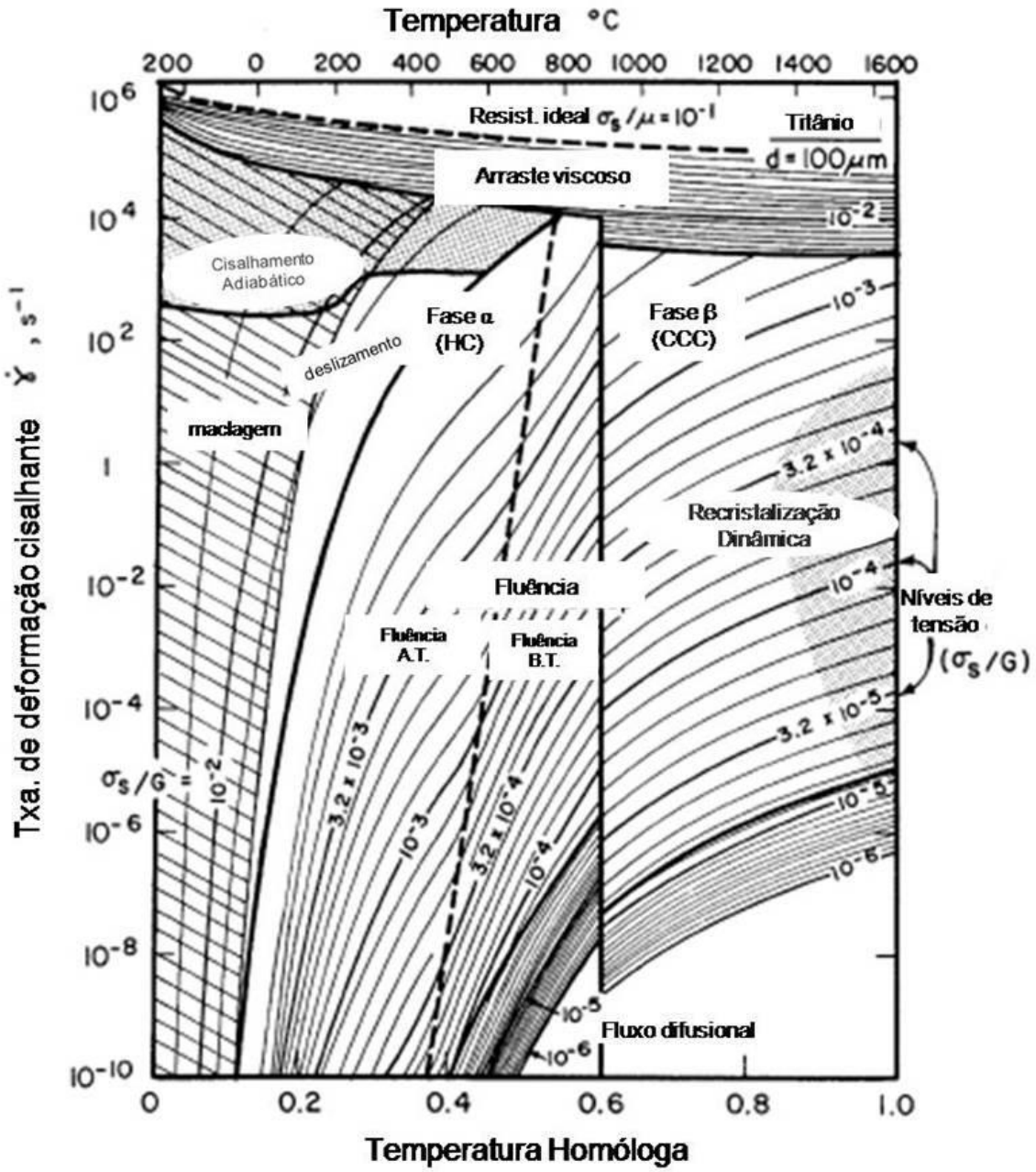

Mechanical Behavior

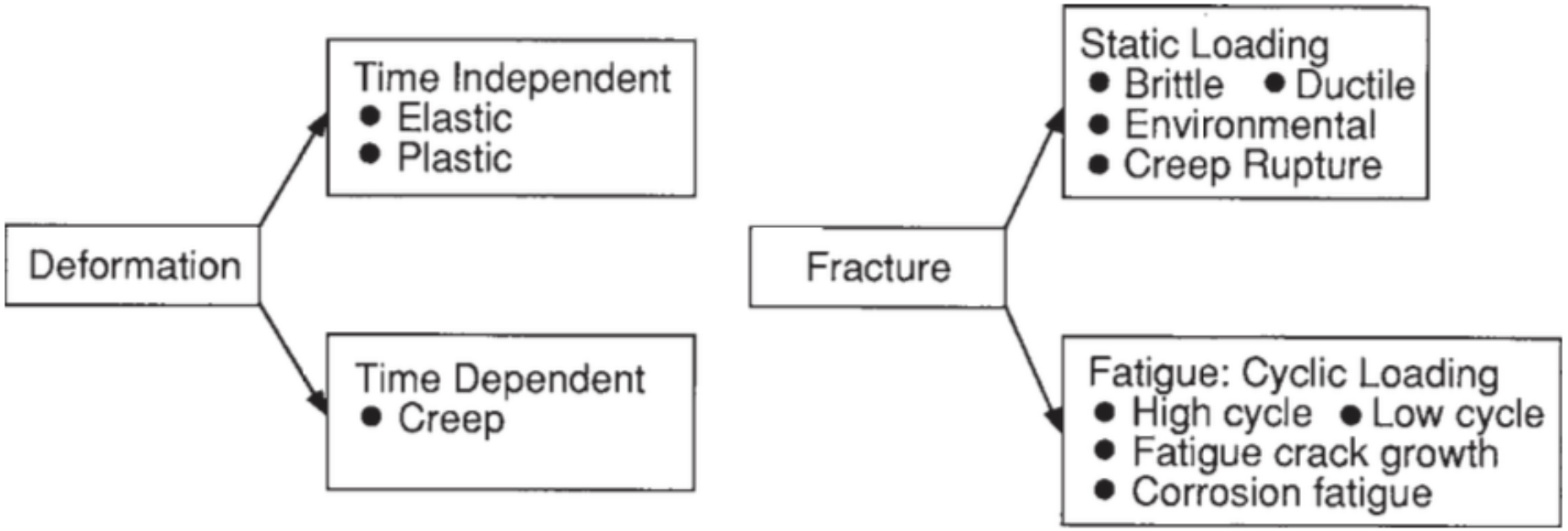

Figure 1.1 Basic types of deformation and fracture.

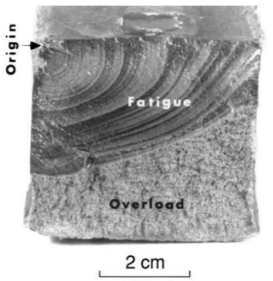

Figure 9.21 Fracture surfaces for fatigue and final brittle fracture in an 18 Mn steel member. (Photo courtesy of A. Madeyski, Westinghouse Science and Technology Ctr., Pittsburgh, PA.)

Mechanical Behavior

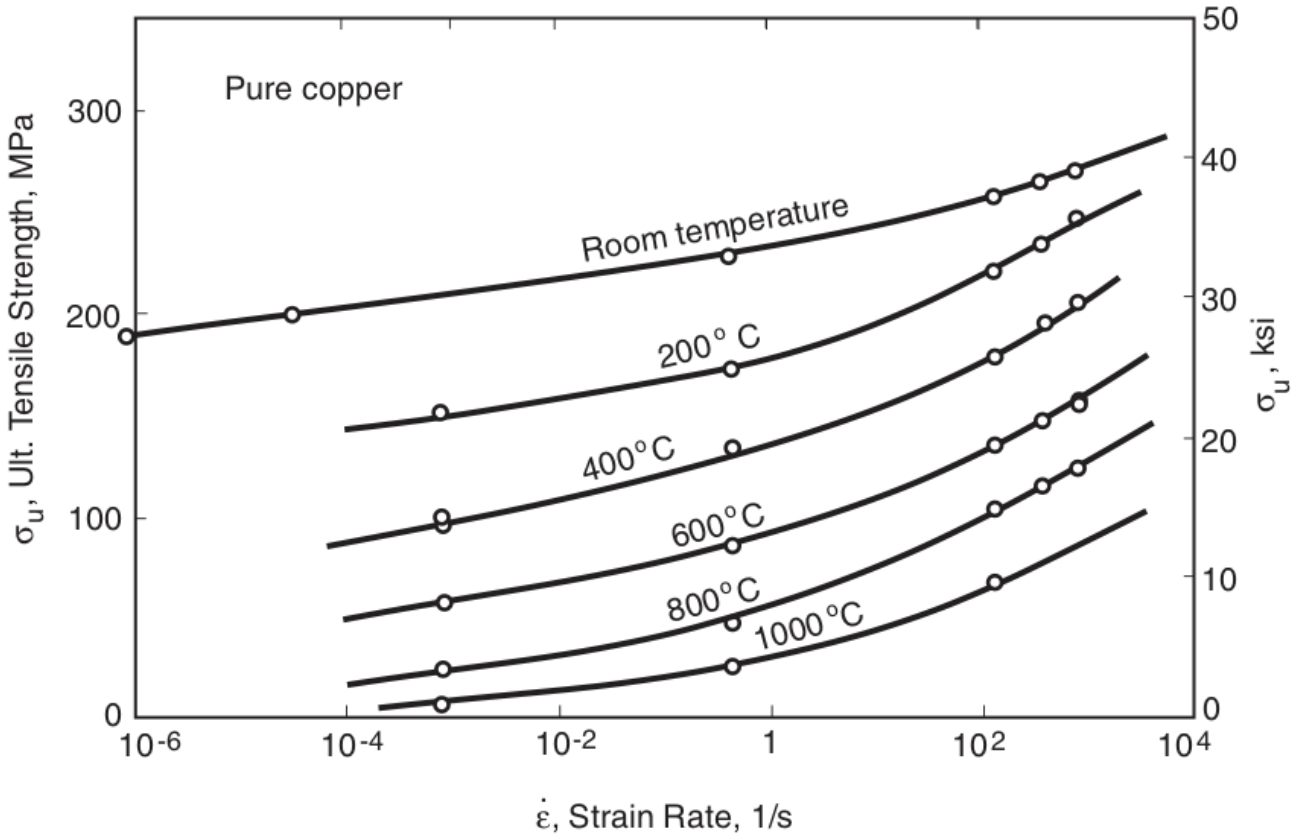

Figure 4.17 Effect of strain rate on the ultimate tensile strength of copper for tests at various temperatures. (Adapted from [Nadai 41]; used with permission of ASME.)

Manufacturing : Requirements and influence

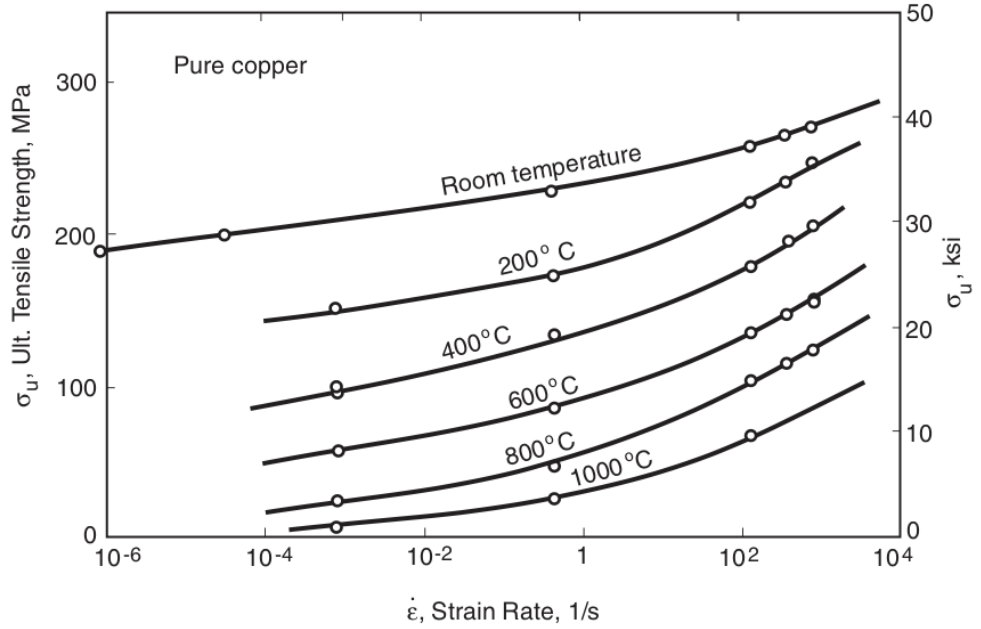

Figure 4.17 Effect of strain rate on the ultimate tensile strength of copper for tests at various temperatures. (Adapted from [Nadai 41]; used with permission of ASME.)

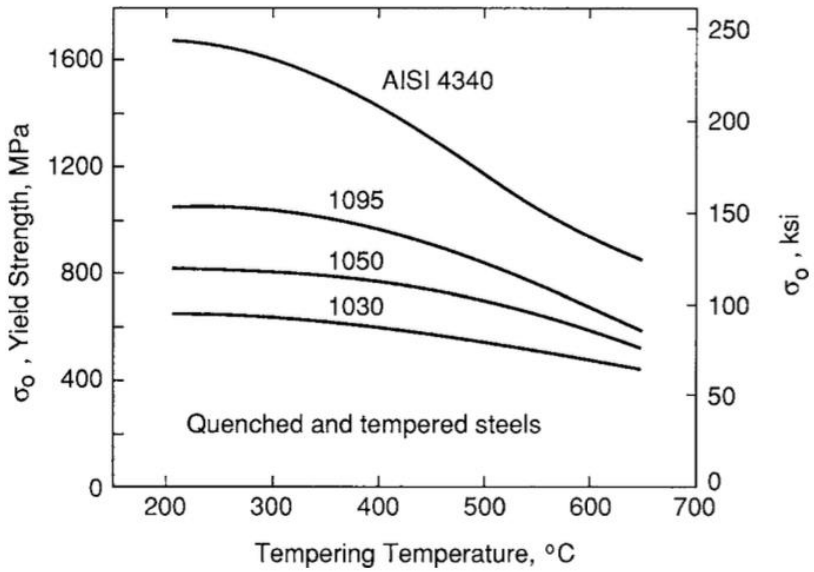

Figure 3.9 Effect of tempering temperature on the yield strength for several steels. These data are for 13 mm diameter samples machined from material heat treated as 25 mm diameter bars. (Data from [Boyer 85] p. 4.21.)

Mechanical behavior

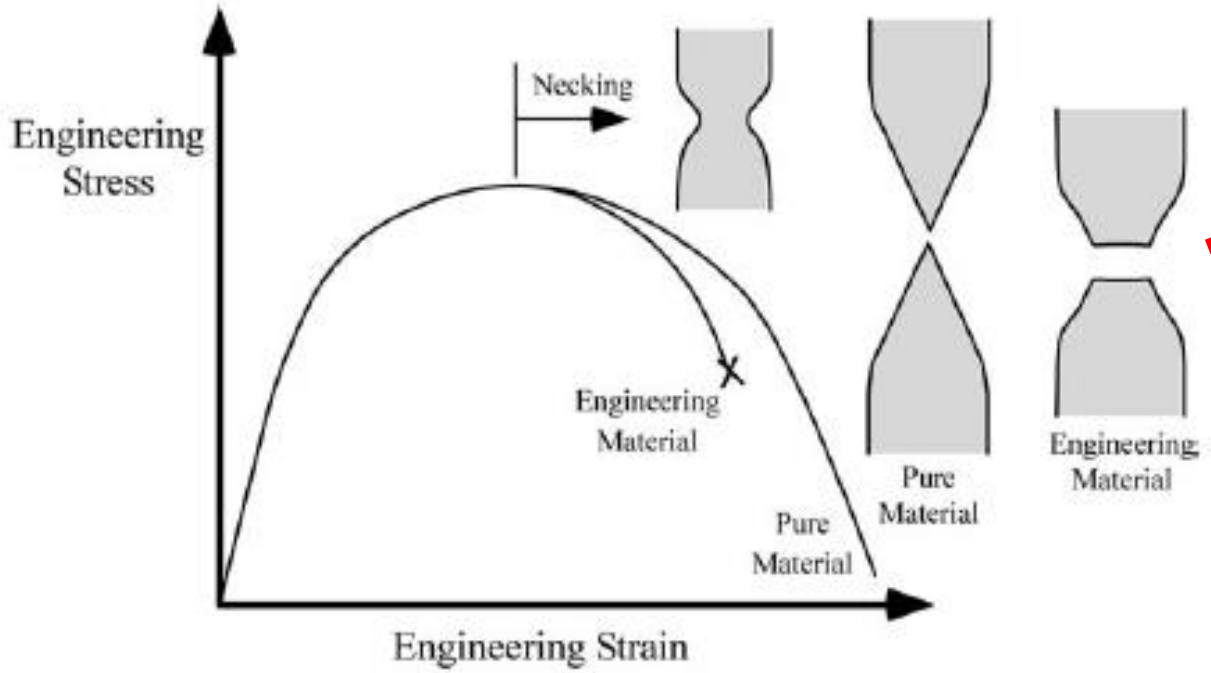

FIGURE 5.2 Uniaxial tensile deformation of ductile materials.

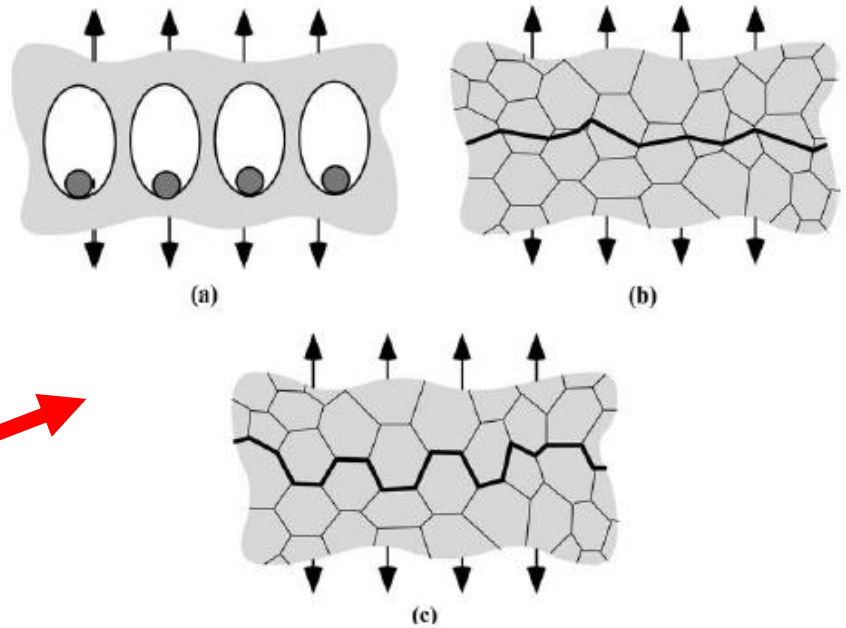

FIGURE 5.1 Three micromechanisms of fracture in metals: (a) ductile fracture, (b) cleavage, and (c) intergranular fracture.

Mechanical behavior

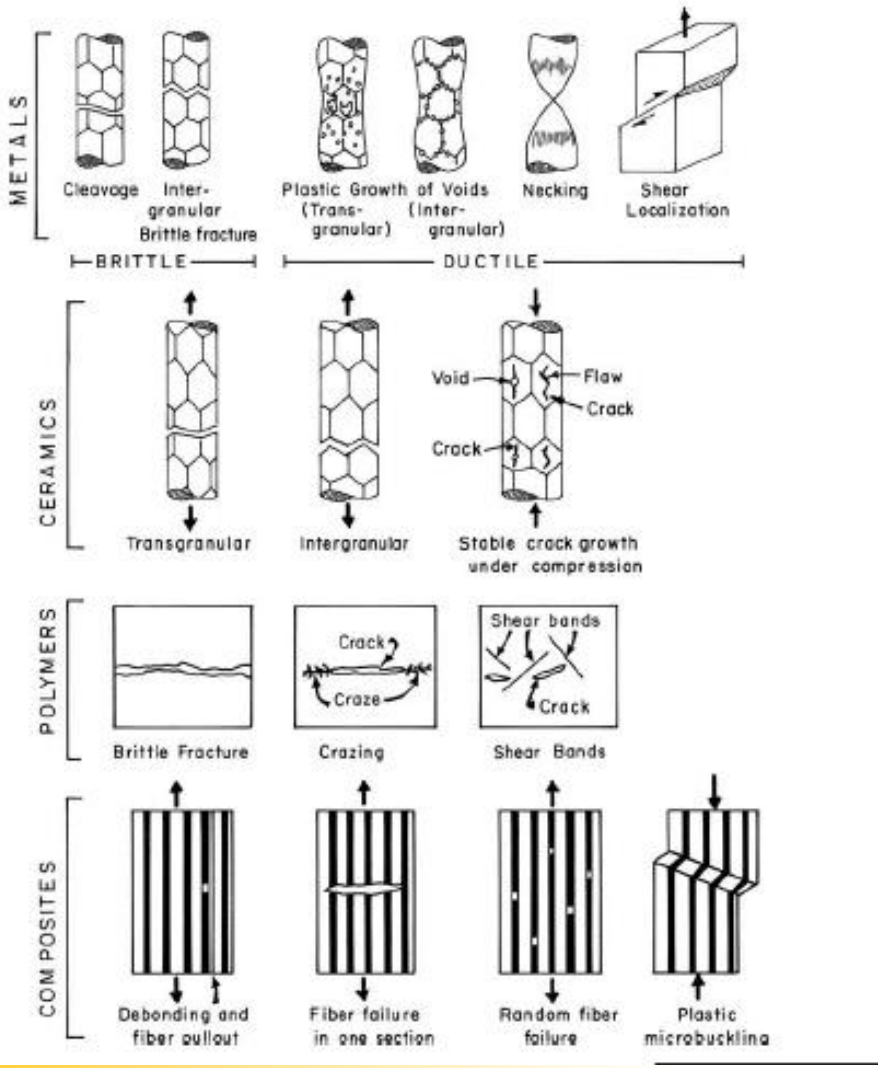

Table 8.1 | Materials of Various Degrees of Brittleness[a]

Type	Principal Factors	Materials
Brittle	Bond rupture	Structures of type diamond, ZnS, silicates, alumina, mica, boron, carbides, and nitrides
Semibrittle	Bond rupture, dislocation mobility	Structures of type NaCl, ionic crystals, hexagonal close-packed metals, majority of body-centered cubic metals, glassy polymers
Ductile	Dislocation mobility	Face-centered cubic metals, some body-centered cubic metals, semicrystalline polymers

[a] Adapted with permission from B. R. Lawn and T. R. Wilshaw, *Fracture of Brittle Solids* (Cambridge, U.K.: Cambridge University Press, 1975), p. 17).

Mechanical behavior

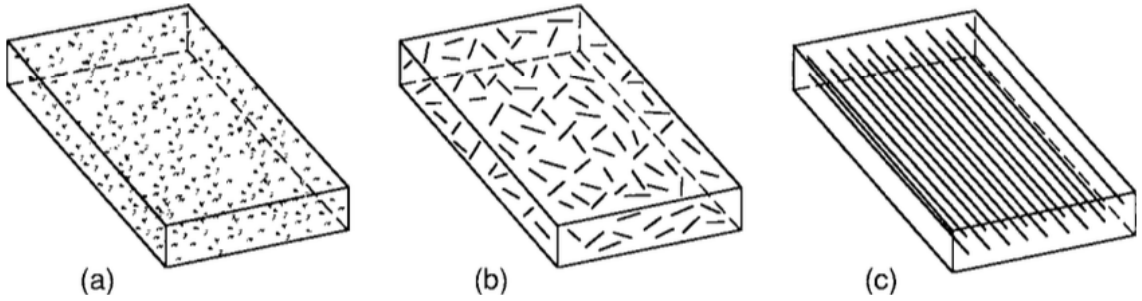

Figure 3.23 Composites reinforced by (a) particles, (b) chopped fibers or whiskers, and (c) continuous fibers. (Adapted from [Budinski 96] p. 121; © 1996 by Prentice Hall, Upper Saddle River, NJ; reprinted with permission.)

Fig. 8.27 Some toughening mechanisms in ceramics.

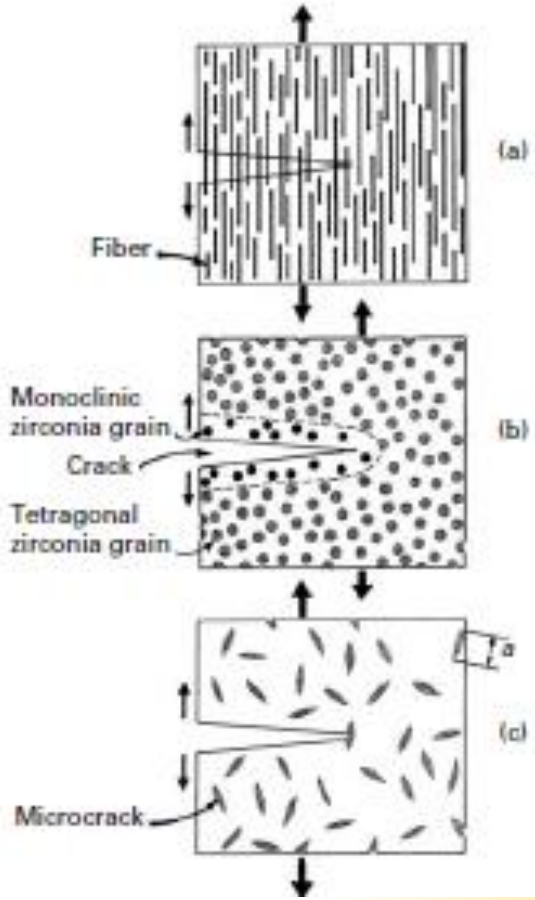

Mechanical Behavior and Microstructural Features

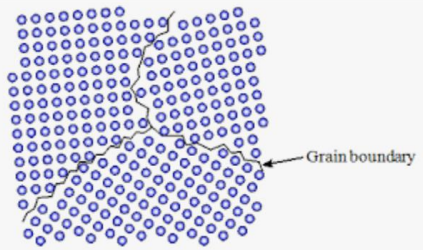

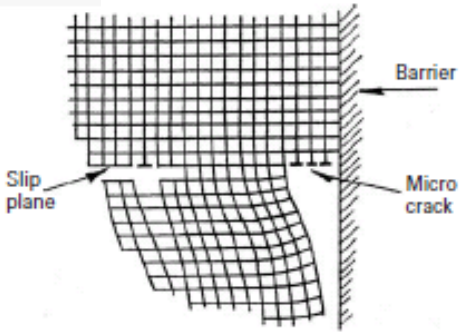

Fig. 8.3 Grouping of dislocations piled up at a barrier and leading to the formation of a microcrack (Zener–Stroh crack).

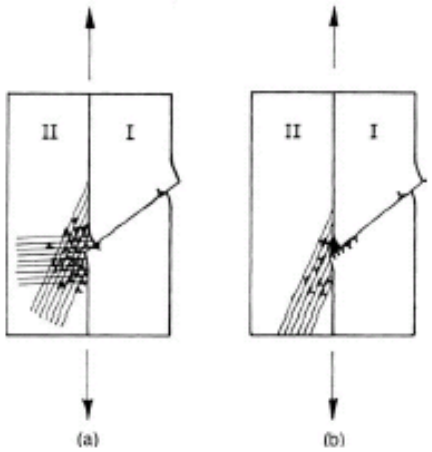

Fig. 8.4 Bicrystal with a slip band in grain I. (a) The stress concentration at the boundary of the barrier due to slip band is fully relaxed by multiple slip. (b) The stress concentration is only partially relaxed, resulting in a crack at the boundary.

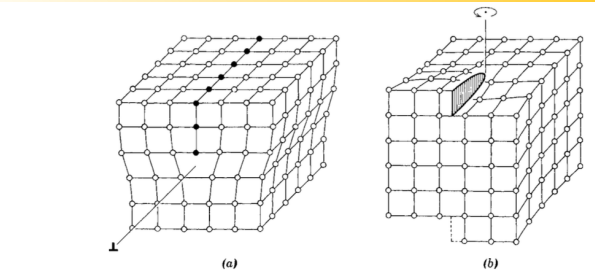

Figure 2.14 The two basic types of dislocations: (a) edge dislocation, and (b) screw dislocation. (From [Hayden 65] p. 63; used with permission.)

Fig. 8.5 Crack nucleation by (a) lattice rotation due to band planes and (b) deformation twins. (c) Crack nucleation in zinc due to lattice rotation associated with band planes. (Reprinted with permission from J. J. Gilman, *Physical Nature of Plastic Flow and Fracture*, General Electric Report No. 60-RL-2410M, April, 1960, p. 83.)

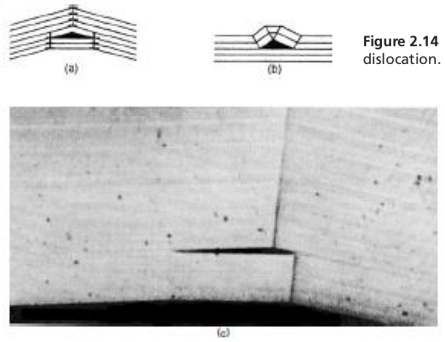

Fig. 8.6 Initiation of failure by microcrack formation in tungsten deformed at approximately $10^4\ s^{-1}$ at room temperature. (a) Twin steps. (b) Twin steps and twin–twin intersection. (From T. Dümmer, J. C. LaSalvia, M. A. Meyers, and G. Ravichandran, *Acta Mater.*, 46 (1998) 959.)

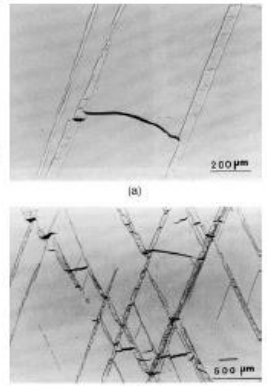

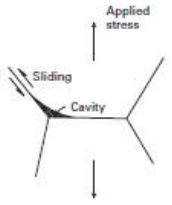

Fig. 8.7 w-type cavitation at a grain-boundary triple point.

development of stress concentrations at grain-boundary triple points (where three grain boundaries meet). Cracks nucleate at such triple points as shown schematically in Figure 8.7. Figure 8.8 shows a micrograph of copper in which such a crack nucleation has occurred. This type of crack is called *w-type cavitation* or *w-type cracking*. Yet

References

DOWLING ,N.E. , KAMPE, S.L., KRAL, M.V. - Mechanical Behavior of Materials (5th Edition) 5th Edition. Pearson. 2018.

ISBN-13: 978-0134606545 and ISBN-10: 013460654X

Marsland, S.- Machine Learning: An Algorithmic Perspective, Second Edition (Chapman & Hall/Crc Machine Learning & Pattern Recognition), 2014. ISBN-13: 978-1466583283 and ISBN-10: 1466583282

MEYERS, M. A. e CHAWLA, K. K. - Mechanical Behavior of Materials, Cambridge University Press, 2009.

ABBASCHIAN, R., REED-HILL, R. E. - Physical Metallurgy Principles 4th Edition, Cengage Learning, 2009, 750p.

ANDRESON, T.L. Fracture Mechanics: Fundamentals and Applications, Third Edition, CRC Press, 2005, 640 p.

DIETER, G. E. - Mechanical Metallurgy, McGraw Hill Book Company , 1988.

HASLACH, H. W.; ARMSTRONG, R.W. Deformable Bodies and Their Material Behavior. USA: John Wiley & Sons. 2004, 531p.

HERTZBERG, R. Deformation and fracture mechanics of engineering materials. John Wiley & Sons, Inc. 1989.

HULL, D., BACON, D.J. Introduction to dislocations. Great Britain:Butterworth- Heinemann. 2011. 257p.

MEYERS, M.A. Dynamic Behavior of Materials. New York: John Wiley & Sons, 1994. 668p.

THEOBALD, O., Machine Learning for Absolute Beginners: A Plain English Introduction, 2018.

MITCHELL, T., Machine Learning, McGraw-Hill, 1997.

HASTIE, T; TIBSHIRANI, R.; FRIEDMAN, J. The Elements of Statistical Learning, 2nd edition, Springer-Verlag, 2009.

Comment: Pictures and Figures were from DOWLING, MEYERS, ASHBY and google search